Megascolides-1
PEP-162 onshore Gippsland Basin

A discussion of the possible thermal and burial histories based on vitrinite reflectance results and recommendations for follow-up studies

GEOTRACK REPORT #938

Report prepared for Karoon Gas Pty Ltd

Report prepared by: I. R. Duddy

June 2005

Geotrack International Pty Ltd ABN 16 006 821 209
37 Melville Road, Brunswick West, Victoria 3055, Australia Ph +613 9380 1077 facsimile +61 3 9380 1477
email mail@geotrack.com.au

Megascolides-1
PEP-162 onshore Gippsland Basin

A discussion of the possible thermal and burial histories based on vitrinite reflectance results and recommendations for follow-up studies

GEOTRACK REPORT #938

CONTENTS

TABLES

CONTENTS (Continued)
TABLES

FIGURES

Megascolides-1
PEP-162 onshore Gippsland Basin

A discussion of the possible thermal and burial histories based on vitrinite reflectance results and recommendations for follow-up studies

GEOTRACK REPORT #938

EXECUTIVE SUMMARY

Introduction and Objectives

This report provides a discussion of possible thermal and burial history reconstructions of the Megascolides-1, PEP-162, onshore Gippsland Basin, based on vitrinite reflectance data (VR). The study was commissioned by Mark Smith for **Karoon Gas Pty Ltd** who supplied all of the data used in this report. This report was completed in June 2005. The VR data have been used to identify any episodes of heating and cooling which have affected the section intersected in this well.

SUMMARY CONCLUSIONS

The Megascolides-1 well intersected a thin ?Oligocene volcanic and clastic sequence unconformably overlying the Early Cretaceous Strzelecki and Crayfish groups with TD at 2000 mbRT in volcanics attributed to the Duck Bay Formation. VR results are available only from the Early Cretaceous sequence from the Megascolides-1 well and these data have allowed constraints on three major aspects of the thermal history:

1. The maximum paleotemperatures reached by the Early Cretaceous sequence – indicating ~46 to 74°C of cooling has occurred (Table i).
2. The paleogeothermal gradient at the time of maximum paleotemperatures – which is just consistent with the present day geothermal gradient of 43.3°C/km at the limits of the data (~16.5 to 42.5°C/km; Table ii; Figure 2.4).
3. The magnitude of burial at the time of maximum paleotemperatures – within the range 1500 to 5750 m at ±95 confidence limits (Table iii).

However, it has not been possible to provide rigorous constraints on the timing of any thermal episodes that may have affected the drilled Tertiary and Early Cretaceous sequences, and in particular, the time of maximum paleotemperatures is not known and must be assumed.

Geotrack International Pty Ltd ABN 16006 821 209
37 Melville Road, Brunswick West, Victoria 3055 Australia tel: +613 9380 1077 fax: +613 9380 1477

email: mail@geotrack.com.au website: www.geotrack.com.au

A number of alternative thermal and burial histories for the Megascolides-1 well are discussed with variation in the time of maximum paleotemperatures based on our regional knowledge and as illustrated in Figure i. Reconstructions 2 and 4, or variations of these, with the time of maximum paleotemperatures assumed to have occurred at either 95 or 80 Ma, or both, are considered the most geologically reasonable. Alternatives with a more recent heating event at some time in the Tertiary have not been pursued, but are also possible on the basis of the available data. Furthermore, we speculate that the present-day geothermal gradient of 43.3°C/km derived from the corrected BHT data is anomalous, either because it has been overcorrected, or it has increased to the measured level only in the very recent geological past (< 1 million years, say).

Recommendations

1. In order to specifically address the question of the time of heating a program of AFTA (apatite fission track analysis) is recommended from the Megascolides-1 well, with 5 samples taken from the Early Cretaceous Strzelecki and Crayfish groups. Application of AFTA will also enable direct assessment to be made of the duration of the present-day geothermal gradient of 43.3°C/km.present-day geothermal gradient of 43.3°C/km.

2. One or two additional VR samples from the Childers Fm clastic sequence is recommended in order to provide some simple constraints on the post-Oligocene thermal history that are currently available. The proposed AFTA sampling from the Early Cretaceous sequence will also provide direct constraints on the timing of any post-Oligocene heating should it be present.

3. Additional biostratigraphic determinations should also be attempted on the Childers Fm clastic sequence to establish the depositional age of this sequence.

Table i: Paleotemperature analysis summary: VR data from the Megascolides-1 well, Gippsland Basin, Australia (Geotrack Report 938)

Depth (m)	Sample type	Present temperature[*1] (°C)	Stratigraphic Unit	Stratigraphic Age (Ma)	VR (%$R_o$max)	Maximum paleotemperature[*2] (°C)
240	cuttings	25	Strzelecki Group- C. striatus	107-108	0.55	99
685	cuttings	44	Strzelecki Group- C. hughesi	115-108	0.66	116
1019.0	core	59	Strzelecki Group- C. hughesi	115-108	0.71	125
1104.2	core	63	Strzelecki Group- C. hughesi	115-108	0.83	137
1535	cuttings	81	Strzelecki Group- U. F wonth	123-115	0.79	134
1820	cuttings	94	Strzelecki Group- U. F wonth	123-115	0.86	140
1920	core	98	Crayfish Group eq.- U. F wonth	123-115	1.15	160

[*1] Based on a surface temperature of 15°C and present day geothermal gradient of 43.3°C/km derived from the corrected BHT data – (see Appendix A).

[*2] Derived from the VR data using the algorithm of Burnham and Sweeney (1989) and an assumed heating rate of 5°C/Myr and a cooling rate of 10°C/Myr (see Appendix B).

Table ii: Summary of paleogeothermal gradient estimates derived from the VR results in the Megascolides-1 well, Gippsland Basin, Australia (Geotrack Report #938)

WELL	Present-day gradient[*1] (°C/km)	Time of maximum Paleotemperatures (Unknown[*2]) Paleogeothermal gradient[*3] (°C/km)
Megascoloides-1	43.3	29.5 (16.5 – 42.5)

Footnotes:

[*1] Present-day gradients are based on corrected BHT data and a surface temperature of 15°C (see Appendix A).

[*2] Time of cooling from maximum paleotemperatures is unconstrained – application of AFTA is recommended to directly determine this.

[*3] Maximum likelihood value derived from the VR results with 95% confidence interval range in brackets.

Table iii: Summary of Removed section estimates derived from the VR results in the Megascolides-1 well, Gippsland Basin, Australia (Geotrack Report #938)

WELL	Present-day gradient[*1] (°C/km)	Time of maximum Paleotemperatures (Unknown)[*2] Section removed[*3,*4] (m)
Megascoloides-1		2700
		(1500 - 5750)
	43.3	(1450±100)[*5]

[*1] Present-day gradient is based on corrected BHT data and a surface temperature of 15°C (see Appendix A).

[*2] Time of maximum paleotemperatures and therefore maximum maturation is unknown. Application of AFTA could directly determine this timimg

[*3] Total section removed with respect to the top-Strzelecki Group unconformity at a present-day depth of 61 m in this well – see Table A.1 (Appendix A).

[*4] Maximum likelihood value with the 95% confidence interval range in brackets underneath. A paleo-surface temperature of 15°C is assumed at the time of maximum paleotemperatures.

[*5] Values italicised in brackets are amounts of removed section based on a paleogeothermal gradient of 43.3°C/km (equal to the present-day level) at the time of maximum paleotemperatures. Not however, that the control on the present-day geothermal gradient is poor and it may be much lower than estimated – see text for more detail.

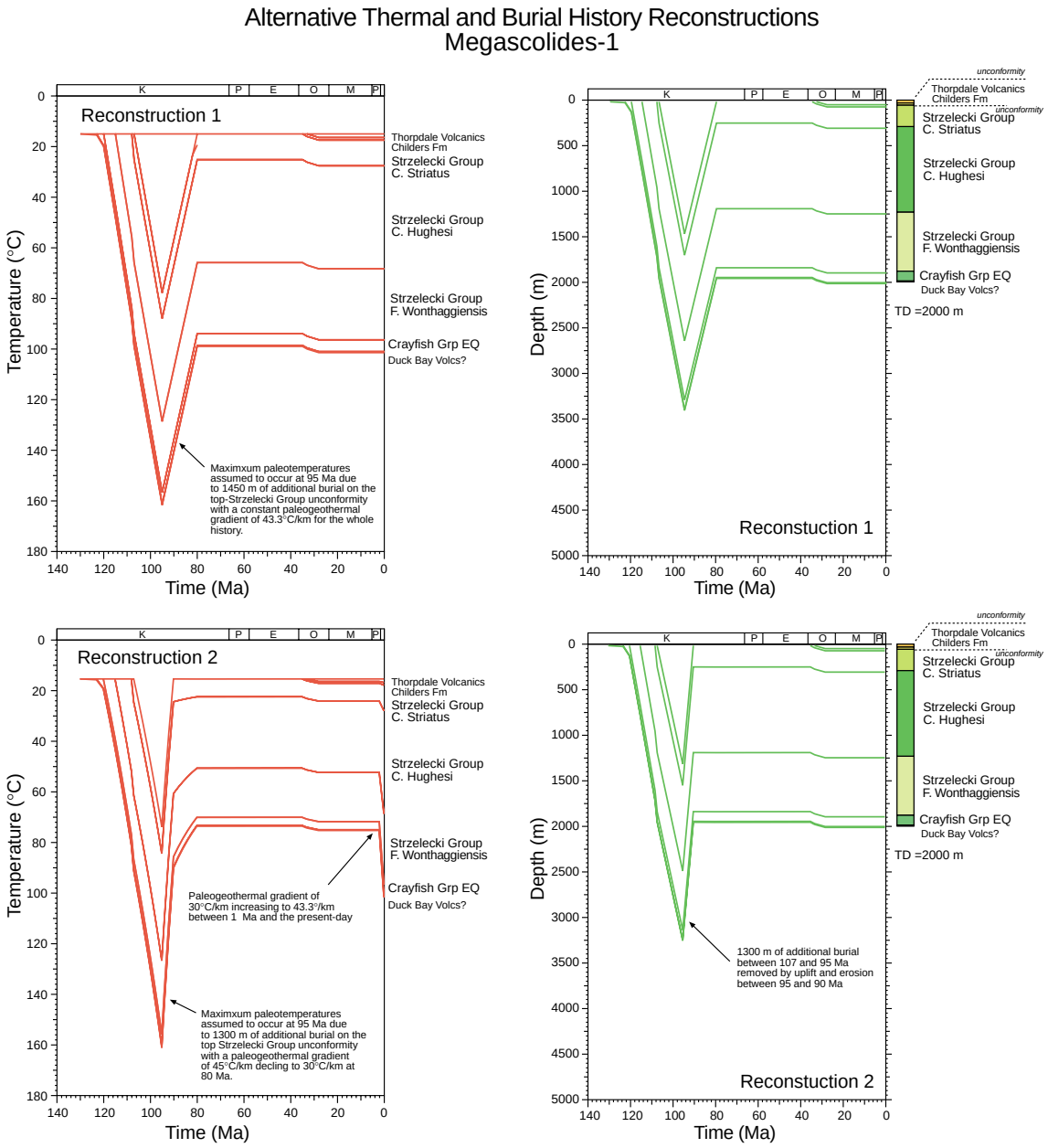

Figure i: Schematic illustration of possible alternative thermal and burial histories derived from the VR results in samples from the **Megascolides-1 well, Gippsland Basin.** Thermal history constraints from individual VR samples are presented in Table i, with formal estimates of paleogeothermal gradient in Table ii and estimated for removed section in Table iii.

Reconstruction 1: Geothermal gradient of 43.3°C/km for the whole history with 1450 m of additional Strzelecki Group section deposited between 107 and 95 Ma and eroded between 95 and 80 Ma.

Reconstruction 2: Geothermal gradient increasing from of 30°C/km at 135 Ma to 45°C/km at 95 Ma and declining to 30°C/km at 80 Ma, remaining at this level until 1 Ma then increasing to 43.3°C/km at the present day combined with 1300 m of additional Strzelecki Group section deposited between 107 and 95 Ma and eroded between 95 and 80 Ma.

Reconstructions 2 and 4, or variations of these, are considered to be more geologically realistic, but without some direct information on the timing of heating, they should all be regarded as highly speculative. In particular, alternative histories with a more recent heating event at some time in the Tertiary have not been pursued, but are also possible on the basis of the available data.

Figure i continued over page.

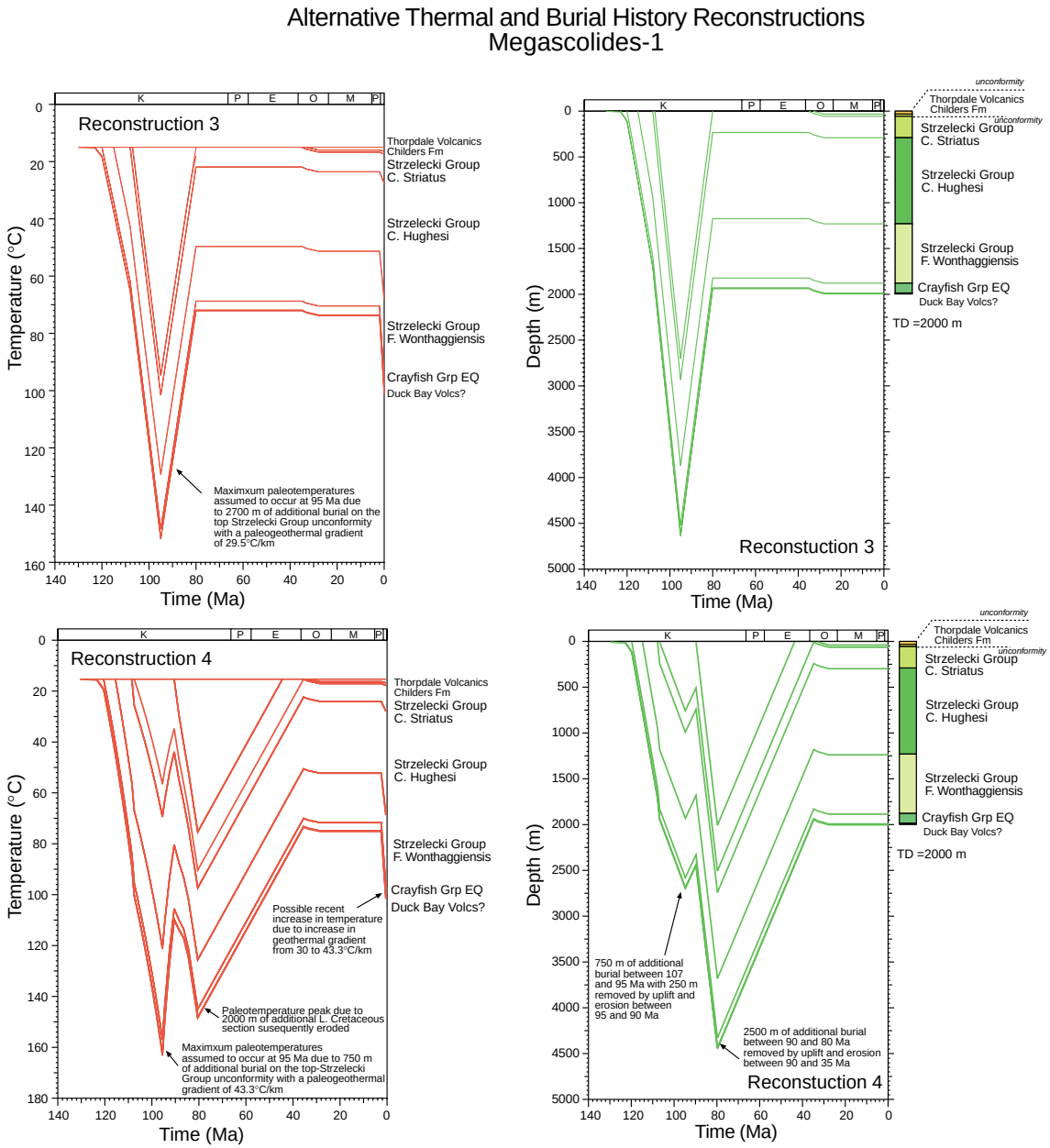

Figure i (cont): Schematic illustration of possible alternative thermal and burial histories derived from the VR results in samples from the **Megascolides-1 well, Gippsland Basin.** Thermal history constraints from individual VR samples are presented in Table i, with formal estimates of paleogeothermal gradient in Table ii and estimated for removed section in Table iii.

Reconstruction 3: Geothermal gradient of 29.5°C/km from 135 Ma to 1 Ma increasing to 43.3°C/km at the present day. 2700 m of additional Strzelecki Group deposited between 107 & 95 Ma and eroded between 95 & 80 Ma.

Reconstruction 4: Geothermal gradient increasing from 29.5°C/km at 135 Ma to 55°C/km at 95 Ma and declining to 29.5°C/km at 80 Ma, remaining at this level until 1 Ma then increasing to 43.3°C/km at the present day. This is combined with deposition of 750 m of additional Strzelecki Group section between 107 and 95 Ma, 250 m of which is eroded between 95 and 90 Ma, followed by deposition of 2000 m of Late Cretaceous section between 90 and 80 Ma with 2500 of section eroded between 80 and 35 Ma.

Reconstructions 2 and 4, or variations of these, are considered to be more geologically realistic, but without some direct information on the timing of heating, they should all be regarded as highly speculative. In particular, alternative histories with a more recent heating event at some time in the Tertiary have not been pursued, but are also possible on the basis of the available data.

1. Introduction

1.1 Aims and objectives

This report provides a discussion of possible thermal and burial histories reconstruction study of the Megascolides-1, PEP-162, onshore Gippsland Basin (Figure 1.1), based on vitrinite reflectance (VR) data. The study was commissioned by Mark Smith for **Karoon Gas Pty Ltd**, who supplied all of the data used in this report. This report was completed in June 2005. The VR data have been used to identify any episodes of heating and cooling which have affected the section intersected in this well.

1.2 Basic data

Formation tops, Cretaceous palynology and present-day temperature data from the Megascolides-1 well (Tables A.1 and A.2, Appendix A) together with a suite of 7 VR determinations from the Early Cretaceous section (Table D.2, Appendix D) were supplied for the study by the client. The VR data was provided to the client by Geotech Pty Ltd and was ultimately commissioned from Prof. Alan Cook of Keiraville Konsultants Pty Ltd.

1.3 Data quality

VR data

The quality of the vitrinite reflectance analyses carried out by Keiraville Konsultants for this report is considered to be generally excellent. Measurement of a total of 25 fields or more is usually considered desirable for an analysis of the highest quality. This "target" was achieved in five of the seven samples from the Megascolides-1 well and the two remaining samples provided 4 and 6 VR measurements (Table D.2, Appendix D). A mean value based on 10 or more measurements is considered very reliable because of the way in which the VR data are gathered, with primary in-situ vitrinite identified on petrographic grounds within polished sections (see Appendix D).

Organic macerals, other than vitrinite, mainly inertinite, were measured in some samples (see summaries in Table D.2 and detailed results and maceral descriptions in

Appendix D), and this can be used to provide alternative maturity estimates as discussed in the text.

Overall, these VR results and considered to be of high quality and they provide a coherent maturity profile for the drilled Early Cretaceous section of each well.

1.4 Report structure

The main conclusions of this report are provided in the Executive Summary. A summary of the thermal history interpretation of the VR data in individual samples from the Megascolides-1 well is provided in Table i, while Table ii summarises constraints on the paleogeothermal gradient at the time of maximum paleotemperatures and Tables iii summarises constraints on the amounts of missing section associated with this paleothermal episode. Figure i provides schematic illustrations of the likely range of thermal history interpretations of the results.

The principles of interpretation of AFTA and VR data are briefly explained in Appendices B and C).

Introductory aspects of the report are dealt with in Section 1, including comments on data quality. Section 2 presents an analysis of the VR supplied by the client using Geotrack's Default History approach together with an assessment of the range of possible thermal and burial histories consistent with the data and our knowledge of the regional thermal history. Recommendations for further work to improve the understanding of the region are provided in Section 3.

Supporting information and data are provided in four Appendices (A, B, C, and D). Appendix A contains the supporting geological information including stratigraphy of the section intersected in the well together with measured BHT data and details of the corrected present-day temperature results. The principles of interpretation of AFTA and VR data are briefly explained in Appendix B. Appendix C outlines the principles employed in interpreting the AFTA and data in terms of thermal history. The VR data and detailed organic maceral descriptions by Keiraville Konsultants and supplied by the client for this study are summarised in Appendix D, which also discusses the principles involved in integrating AFTA and VR data to provide coherent thermal history interpretations.

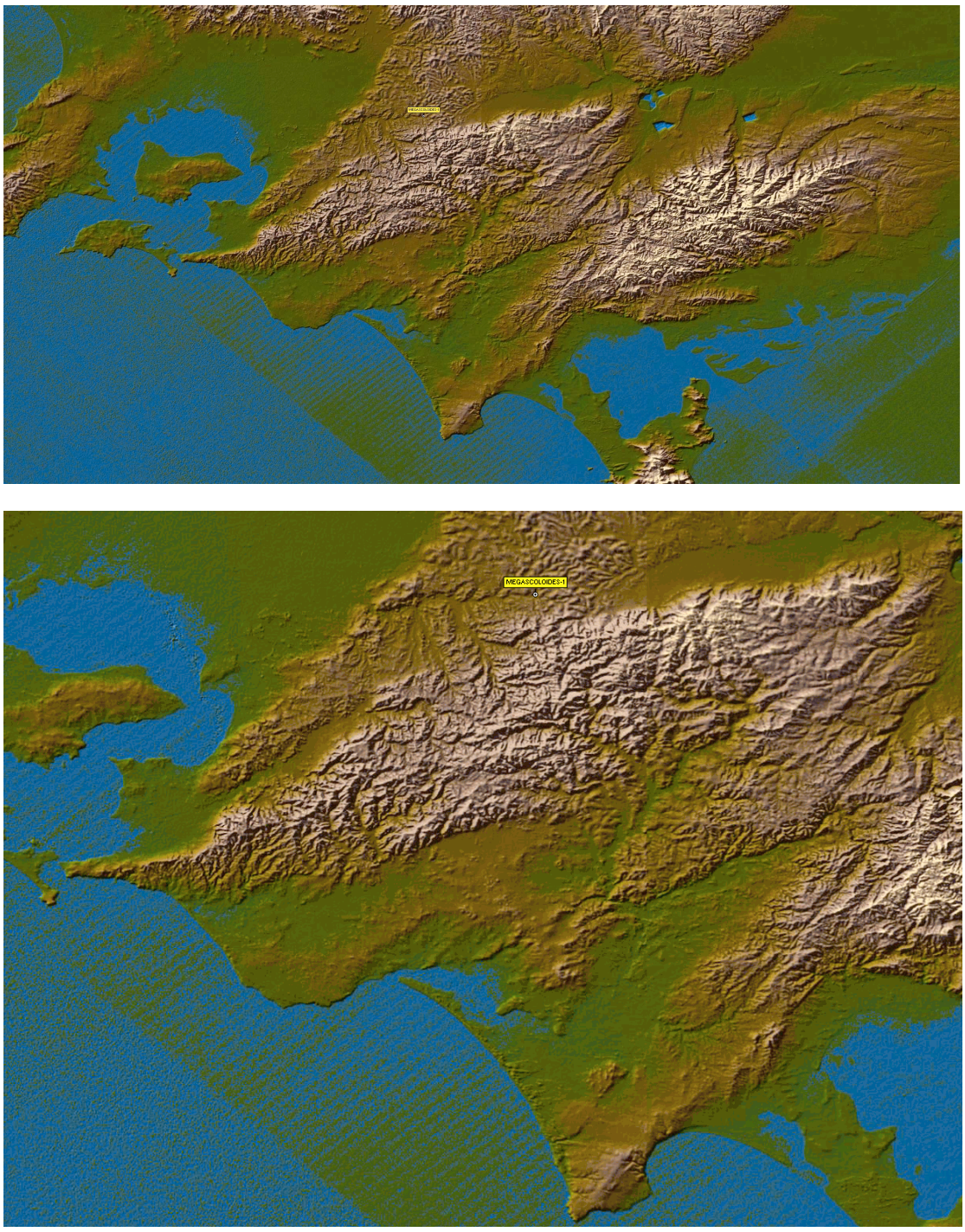

Figure 1.1: Shuttle radar image of southwest Gippsland showing Megascolides-1 well location in relation to the Narracan lobe of the Strzelecki Ranges.

2. Thermal history interpretation of VR data in the Megascolides-1 well

2.1 Introduction

The **Megascolides-1 well** was drilled in the onshore Gippsland Basin just to the north of the Narracan Lobe of the Strzelecki Ranges (Figure 1.1). Information supplied by the client indicates that the well intersected the Thorpdale volcanics (?Oligocene age) at surface overlying a thin clastic sedimentary sequence attributed to the Childers Fm (Barracouta Fm equivalent), which has been assumed here to be of Oligocene age. The Oligocene sequence unconformably overlies the Early Cretaceous Strzelecki Group sedimentary sequence at 61 m, including sediments equivalent to the Crayfish group at 1883 m, bottoming in 58 m of volcanics attributed to the Duck Bay volcanics, with TD at 2000 mrKB. The detailed stratigraphic succession in this well is summarised in Table A.2. The estimated present-day geothermal gradient for the well is 43.3°C/km, based on correction to a single BHT value provided by the client (Table A.3), combined with a surface temperature of 15°C. For a number of reasons this present-day gradient is considered to be anomalously high as discussed below.

Vitrinite reflectance analyses were supplied on 7 samples from the Early Cretaceous sequence of the **Megascolides-1 well** (Table D.2, Appendix D), and together with the stratigraphic information, these VR results provide the basis for the analysis of the thermal and burial histories presented below.

2.2 Thermal history interpretation of VR data

Introduction

Measured vitrinite reflectance data and equivalent VR (VRE) values derived from inertinite reflectance from **Megascolides-1** are summarised in Table 3.1 (see Appendix D for full details) and are plotted against depth below KB in Figure 2.1. Also shown in Figure 2.1 is the VR profile predicted on the basis of the Default Thermal History - i.e. the thermal history predicted for samples from this well if they have never been hotter than their present temperatures at any time in the past, as defined in Section A.1. This history is based on the burial history derived from the units intersected in the well as shown in Figure 2.2, combined with the present-day thermal gradient of 43.3°C/km derived from corrected BHT values and a surface temperature of 15°C, as described in Appendix A.

Evidence from the VR data that the samples have been hotter in the past

All measured VR and VRE values from the Early Cretaceous Strzelecki and ?Crayfish group sequences plot significantly above the VR profile predicted by the Default Thermal History (Figure 2.1), clearly showing that this part of the drilled section has cooled from maximum post-depositional temperatures much higher than the present temperatures at some time since the Early Cretaceous. No VR data is available from the Childers Fm sedimentary sequence below the Thorpdale volcanics so no further information is available to provide any tighter limits on the timing of maximum paleotemperatures.

Further, the trend of the measured VR and VRE data plotted in Figure 2.1 appears to be shallower than the predicted profile which suggests that the paleogeothermal gradient during the heating event responsible for organic matter maturation was lower than the present-day value. A quantitative analysis of paleogeothermal gradients is presented in Section 2.3.

Magnitude of paleotemperatures from VR and the paleotemperature-depth profile in the Megascolides-1 well

Maximum paleotemperatures derived from the measured VR values in this well, using the strategy outlined in Section A.2 (Appendix A) are summarised in Table i (Executive Summary). Values are available over around 1700 m of the Early Cretaceous sequences, and vary from 99 to 160 °C with increasing depth as shown in Figure 2.3. Note that maximum paleotemperature have only been estimated from the measured VR data and not VRE from inertinite as we generally consider the latter estimates to be less reliable than those from true vitrinite and in this case sufficient actual VR data are available to define the shape of the paleotemperature profile.

The maximum paleotemperature estimates define a linear profile significantly above the present-day temperatures profile and with a slope that appears to be somewhat shallower than the present day temperature profile. This suggests that the paleogeothermal gradient at the time of maximum paleotemperatures was lower than the present-day value, as previously noted by inspection of the VR-depth plot in Figure 2.1. A notional paleotemperature profile that honours the key constraints derived from the VR results is shown by the dashed line in Figure 2.3.

A quantitative analysis of the paleogeothermal gradient and its significance in terms of the underlying mechanisms of heating and cooling are discussed in Section 2.3.

2.3 Quantification of paleogeothermal gradients

Using the approach outlined in Section A.4 (Appendix A) and methods explained in Section C.9 (Appendix C), we have determined the range of paleogeothermal gradients consistent with the maximum paleotemperature constraints from the VR data at the time of maximum paleotemperatures. All paleotemperature estimates used in the calculations are summarised in Table i, Executive Summary.

Fitting a line to the profile of maximum paleotemperature estimates from the VR data for this event gives a maximum likelihood estimate of 29.5°C/km and a well-constrained allowed range of paleogeothermal gradient from 16.5 to 42.5°C/km at 95% confidence limits (upper left in Figure 2.4). Results are listed in Table 2.2.

At face value, the allowed range of paleogeothermal gradient *at the time of maximum paleotemperatures* is wholly lower than the present-day gradient of 43.3°C/km derived from the corrected BHT data confirming the qualitative assessment if the results presented in Section 2.2. However, in the two dimensional analysis of paleogeothermal gradient and removed section the upper limit of paleogeothermal gradient is slightly higher at 45°C/km (see the cross plot in Figure 2.4) and this just exceeds the present-day gradient of 43.3°C/km.

Thus, at the very limits of the data, it is possible that the observed heating can be explained solely by deeper burial with the heat flow at the time of maximum paleotemperatures similar to that at the present-day. Further, the results preclude any significant contribution to the heating by increased basal heat flow. It is emphasised however, that without direct information on the time of heating other explanations for the heating may be possible. Some further comments on this aspect of the results are provided in Figure 2.5.

2.4 Quantification of removed section

In this Section, we calculate the amount of additional section that must have been deposited and subsequently removed by uplift and erosion in order to explain the observed paleotemperatures, given the constraints on paleogeothermal gradients established in Section 2.3. We do not necessarily suggest that such an interpretation is preferred over other possible scenarios, but the calculations presented here provide a quantitative framework in which these aspects of the results can be assessed.

Assuming that the paleogeothermal gradient was linear throughout the entire section at the time of maximum paleotemperatures, extrapolation of the fitted linear profile

from the appropriate unconformity to an assumed paleo-surface temperature provides an estimate of the amount by which that unconformity surface was more deeply buried, and hence the amount of section that has since been removed by erosion.

As emphasised in Section A.4, estimation of amounts of removed section from paleotemperature data depends critically on various key assumptions. The principal difficulty lies with definition of the paleogeothermal gradient through the removed section, which cannot be constrained by direct measurement and must therefore always be assumed. In deriving estimates of removed section for each of the paleo-thermal episodes recognised in the well, the paleogeothermal gradient through the removed section is assumed to have been linear and equal to the value through the preserved section. This assumption may be invalid if the elevated paleotemperatures are caused by processes involving lateral or local introduction of heat, such as by confined fluid flow or igneous intrusions.

A constant paleo-surface temperature of 15°C (equivalent to the present-day value) has been assumed in order to estimate amounts of removed section. This is a convenient simplifying assumption, and changing the value of paleo-surface temperature is equivalent to a constant offset in the amount of missing section required in order to explain the observed paleotemperatures. The influence of this factor is discussed further at the end of this Section.

Maximum paleotemperature episode

Estimates of the amount of additional section required to explain the maximum paleotemperatures in this well (Table i, Executive Summary) have been calculated with respect to the unconformity at the top of the preserved Strzelecki Group at a depth of 61 mbRT in this well, representing the interval ~107 to 35 Ma (Table A.1, Appendix A).

Given all the assumptions which underlie this analysis, application of the methods described in Section A.4 gives estimates of the amounts of removed section required to explain the observed paleotemperatures as summarised in Table 2.3. Estimates are quoted corresponding to the maximum likelihood estimate of paleogeothermal gradient and related ±95% confidence limits, derived from the likelihood profiles shown in the upper right position in Figure 2.4. In addition, ranges of removed section (again corresponding to ±95% confidence limits) are quoted for various specified values of paleogeothermal gradient within the allowed range of values. These are taken from the lower plot in Figure 2.4, which illustrates the correlation between values of paleogeothermal gradient and removed section allowed by the paleotemperature constraints characterising each episode within ±95% confidence

limits. That is, any set of paired values inside the contoured region of the plot are compatible with the corresponding paleotemperature data at 95% confidence limits, with higher paleogeothermal gradients requiring correspondingly less removed section, and vice versa.

The overall range of allowed values of section removed since the **time of maximum paleotemperatures**, from 1500 to 5700 metres (Figure 2.4, upper right) is quite broad, as a result of the degree of extrapolation required, coupled with the relatively small depth interval over which data are available. The allowed range of values for removed section defined by the two dimensional analysis in the lower plot in Figure 2.4 is slightly wider overall, from ~1300 to ~7300 metres. But the range of allowed values for fixed values of paleogeothermal gradient is quite narrow (Table 2.3 and lower plot in Figure 2.4). For example, for a paleogeothermal gradient of 43.3°C/km, equal to the present-day value (equivalent to a scenario involving no change in basal heat flow since the time of maximum paleotemperatures), a range of 1350 to 1550 metres of removed section is defined from the results in the Megascolides-1 well.

It is significant that the results allow a maximum paleogeothermal gradient of ~45°C/km at the time of maximum paleotemperatures, which must be coupled with the minimum magnitude of deeper burial of ~1300 m in order to explain the observed heating.

Application of these constraints allows the construction of some speculative thermal and burial histories as presented in Section 2.5.

Changes in paleo-surface temperature

Note that use of a paleo-surface temperature of 15°C is a convenient simplification based on the present-day surface temperature, and it is possible that higher or lower values may be more appropriate. Detailed discussion of this issue is beyond the usual scope of studies such as this, but the magnitude of removed section required to explain the observed paleotemperatures can be easily adjusted to an alternative paleo-surface temperature by subtracting or adding the difference in depth equivalent to the change in paleo-surface temperature, for the appropriate paleo-gradient, as described in Section A.4. For example, increasing the paleo-surface temperature by 10°C, for a paleogeothermal gradient of ~40°C/km, would require a reduction of 250 metres in the amount of removed section needed to explain the observed paleotemperatures.

2.5 Thermal and burial history synthesis

Introduction

The VR results available from the Early Cretaceous sequence from the Megascolides-1 well have allowed constraints on three major aspects of the thermal history:

1. The maximum paleotemperatures reached by the Early Cretaceous sequence
2. The paleogeothermal gradient at the time of maximum paleotemperatures (with some caveats – see below).
3. The magnitude of burial at the time of maximum paleotemperatures.

However, as only VR results are available, it has not been possible to provide rigorous constraints on the timing of any thermal episodes that may have affected the drilled Tertiary and Early Cretaceous sequences. For example, regional thermal history information suggests up to three thermal episodes (note: "thermal episode" is used generically to represent heating by any mechanism – e.g. burial, hot fluids, increase in basal heat flow etc) may have affected the Cretaceous sequence, and the VR data has only provided some constraints on one of these episodes.

Unfortunately, the time of maximum paleotemperatures is not known and must be assumed and in the following discussion, we provide some possible thermal and burial histories reconstructions based on the VR results and incorporating timing information based on the regional thermal history obtained from previous studies in the broader region.

Possible thermal and burial history reconstructions

Reconstruction 1: The simplest interpretation of the VR results is that the geothermal gradient at the time of maximum paleotemperatures was the same as that at the present-day (43.3°C/km), as just allowed at the limit of the results. The time of maximum paleotemperatures and maximum burial are assumed to have been synchronous at 95 Ma due to deposition of an additional 1450 m of section on the top-Strzelecki Group unconformity subsequently eroded between 95 and 80 Ma. The remainder of the burial history is based on the preserved thickness of Oligocene classics and the Thorpdale volcanics. The thermal history is shown in Figure 2.5 (upper left) and the corresponding burial history is shown in Figure 2.6 (upper left) while the predicted VR profile and the measured data are compared in Figure 2.7.

Reconstruction 2: The reasonable fit of the measured data and the predicted profile shows that **Reconstruction 1** is possible, but a constant paleogeothermal gradient of 43.3°C/km is probably unreasonable in this area where previous studies have consistently shown evidence for mid-Cretaceous paleogeothermal gradients around 1.5 to 2 times the present-day levels (e.g. Duddy and Green, 1991; Duddy, 1994). At face value this "high mid-Cretaceous heat flow" scenario would appear to be precluded by the results, but we note that the estimated present-day gradient of 43.3°C/km is higher than generally measured in the region, and it is possible that the "true" present-day gradient is lower. In this case it is possible to develop a scenario where the mid-Cretaceous paleogeothermal gradient was around 45°C/km compared to a "true" present-day gradient of 30°C/km. In this scenario, the present-day gradient of 43.3°C/km estimate from the corrected BHT data could still be correct, but has developed only recently perhaps due to hydrodynamic effects and flow of heated water in shallow aquifer horizons. Alternatively, the single measured BHT value may be incorrect. In either case, further analysis of the present-day thermal regime is warranted and this could be achieved by analysis of AFTA

Thermal History Reconstruction 2 is also shown in Figure 2.5 (lower left), and is based on a paleogeothermal gradient of 30°C/km at 135 Ma increasing to a peak of 45°C/km at 95 Ma declining to 30°C/km at 80 Ma, staying constant at this level until 1 Ma, then increasing to 43.3°C/km at the present day. The corresponding burial history is shown with 1300 m of additional Strzelecki Group section deposited between 107 and 95 Ma and completely eroded between 95 and 80 Ma (Figure 2.6, lower left). The rest of the burial history is the same as used in Reconstruction 1. Again there is a reasonable fit to the VR data (Profile 2), although as might be expected from using a paleogeothermal gradient at the maximum allowed limit, the VR profile lies below the measured data shallow in the section on the high side of the data near TD.

Reconstruction 3: This reconstruction is based on the best-fit values of paleogeothermal gradient of removed section of 29.5°C/km and 2700 m, respectively (Figure 2.4). The history is based on a geothermal gradient of 29.5°C/km that is constant from 135 Ma to 1 Ma increasing to 43.3°C/km at the present day together with 2700 m of additional Strzelecki Group deposited between 107 & 95 Ma and eroded between 95 & 80 Ma. The remainder of the burial history is again based on the preserved thickness of Oligocene classics and the Thorpdale volcanics. The thermal history is shown in Figure 2.5 (upper right) and the corresponding burial history is shown in Figure 2.6 (upper right) while the predicted VR profile (Profile 3) and the measured data are compared in Figure 2.7. This history shows the qualitative

best fit to the measured VR data (Figure 2.7), but is probably the least likely history based on regional thermal history results.

Reconstruction 4: This is the most complex of the thermal histories considered here. It involves a paleogeothermal gradient increasing from of 29.5°C/km at 135 Ma to 55°C/km at 95 Ma and declining to 29.5°C/km at 80 Ma, remaining at this level until 1 Ma then increasing to 43.3°C/km at the present day. This is combined with deposition of 750 m of additional Strzelecki Group section between 107 and 95 Ma, 250 m of which is eroded between 95 and 90 Ma, followed by deposition of 2000 m of Late Cretaceous section between 90 and 80 Ma with 2500 of section eroded between 80 and 35 Ma. The thermal history is shown in Figure 2.5 (lower right) and the corresponding burial history is shown in Figure 2.6 (lower right) while the predicted VR profile and the measured data are compared in Figure 2.7 (VR profile 4).

This complex history has an interesting effect on the maturation history in that the maximum maturity deep in the Strzelecki Group and Crayfish Group developed at 95 Ma while maximum maturity in the shallower Strzelecki Group developed at 80 Ma. This complexity results from the interplay between the elevated mid-Cretaceous paleogeothermal gradient and the deeper Late Cretaceous burial in a lower paleogeothermal gradient regime. This has previously been described as “top-down maturation” (Duddy, 1997) and is a characteristic of Australia’s southern margin Mesozoic-Tertiary sedimentary basins.

Alternatives with a more recent, Tertiary, heating event have not been pursued, but are also possible on the basis of the available data.

Table 2.1: Equivalent VR levels estimated from inertinite reflectance, Megascolides-1 well, Gippsland Basin, (Geotrack Report #938).

Sample Number	Depth (m)	Present temperature[*1] (°C)	Stratigraphic unit	Vitrinite reflectance (%)	Inertinite reflectance (%)	Equivalent vitrinite reflectance[*2] (%)
-	240	25	Strzelecki	0.55	1.41	0.57
-	685	44	Strzelecki	0.66	1.56	0.69
-	1019	59	Strzelecki	0.71	1.54	0.67
-	1104	63	Strzelecki	0.83	-	-
-	1535	81	Strzelecki	0.79	1.66	0.78
-	1820	94	Strzelecki	0.86	1.78	0.90
-	1920	98	Strzelecki (Crayfish Grp)	1.15	1.91	1.04

See Table D.2, Appendix D for full details of vitrinite and inertinite reflectance measurements.

[*1] Based on a present-day gradient of 43.3°C/km.
[*2] In-house Geotrack correlation based on results from Keiraville Konsultants.

Table 2.2: Paleogeothermal gradient estimates, Megascolides-1 well, Gippsland basin (Geotrack Report #938)

Episode	Present-day thermal gradient[*2] (°C/km)	Maximum Likelihood Estimate[*3] (°C/km)	Lower 95% confidence limit[*3] (°C/km)	Upper 95% confidence limit[*3] (°C/km)
Post-Aptian[*1] **(<107 Ma) (VR data only)**	43.3	29.5	16.5	42.5 (46.0)[*4]

[*1] Timing derived solely from the stratigraphic distribution of the VR samples which show the effects of elevated paleotemperatures.

[*2] A present-day thermal gradient of 43.3°C/km has been derived from corrected BHT values as described in Appendix A.

[*3] Paleogeothermal gradients estimated from paleotemperatures derived from the VR data (Table i), using methods described in Appendix B. See Section 3 for details.

[*4] A slightly higher maximum value is allowed by the two-dimensional analysis of paleogeothermal gradient and removed section illustrated in the cross-plot in Figure 2.4.

Table 2.3: Removed section estimates: Megascolides-1 well, Gippsland basin (Geotrack Report #938)

	Estimates of removed section (metres)	
	Post-Aptian [*1] **(<107 Ma)**	**No other episodes defined**
Maximum Likelihood Estimate	2700	-
Lower and upper 95% confidence limits	1500-5750	-
Fixed paleo-geothermal gradients		
10°C/km	*not allowed*	-
15°C/km	6100-6900	-
20°C/km	4150-4950	-
30°C/km	2350-2950	-
40°C/km	1500-1800	-
43.3°C/km	1350-1550	-
45°C/km	~1300	-
50°C/km	*not allowed*	-

[*q] Removed section estimated with respect to the Top-Strzelecki Group unconformity at the a depth of 61 mrKB in this well.

Notes:

Determination of the amount of removed section depends on the assumption that paleogeothermal gradients were linear through both the removed section and the preserved section in the well. This assumption will not be valid if heating involved non-linear paleogeothermal gradients, which may result either because of vertical contrasts in thermal conductivity through the section, or if heating was not directly related to depth of burial but was due e.g. to hot fluid circulation. In such cases, the estimates quoted here are likely to over-estimate true amounts of removed section.

The quoted values are based on an assumed paleo-surface temperature of 15°C for the entire history. These can easily be converted to apply to other values, by subtracting or adding the difference in depth equivalent to the change in paleo-surface temperature, for the appropriate paleo-gradient. For example, for a paleogeothermal gradient of 30°C/km, a decrease of 10°C in the paleo-surface temperature is equivalent to an increase of 333 metres in the amount of removed section.

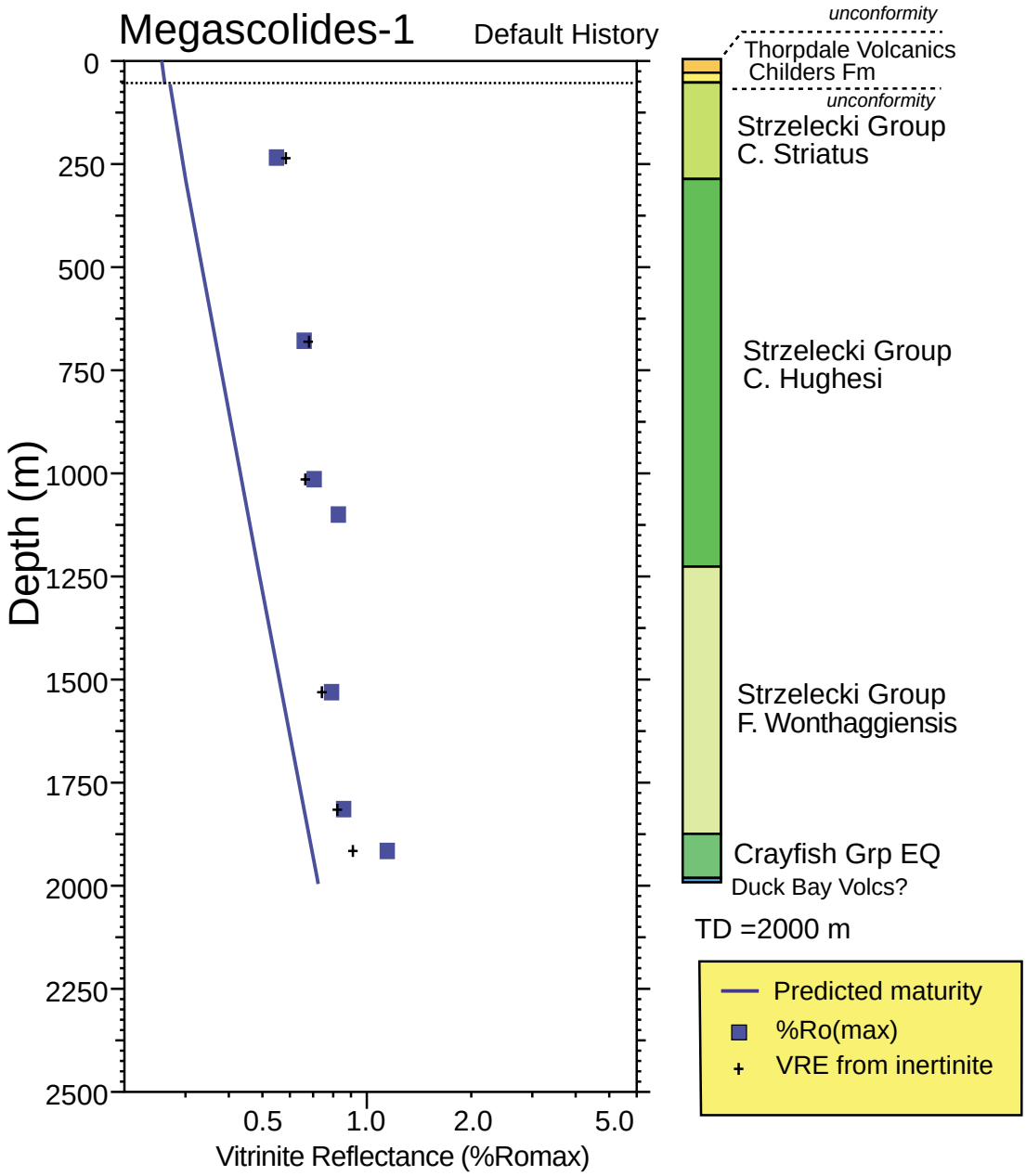

Figure 2.1: Mean vitrinite reflectance values (Table D.2, Appendix D) in the **Megascolides-1 well, Gippsland Basin,** plotted against depth (TVD rkb). Also shown is the profile predicted from the "Default Thermal History", i.e., the profile expected if all units throughout the well are currently at their maximum temperatures since deposition (see Section A.1).

All of the measured VR values plot significantly above the profile predicted by the Default Thermal History, suggesting that the sampled Early Cretaceous units have cooled from maximum post-depositional temperatures significantly higher than the present-day temperatures at some time since deposition of the C. striatus-aged Strzelecki Group section.

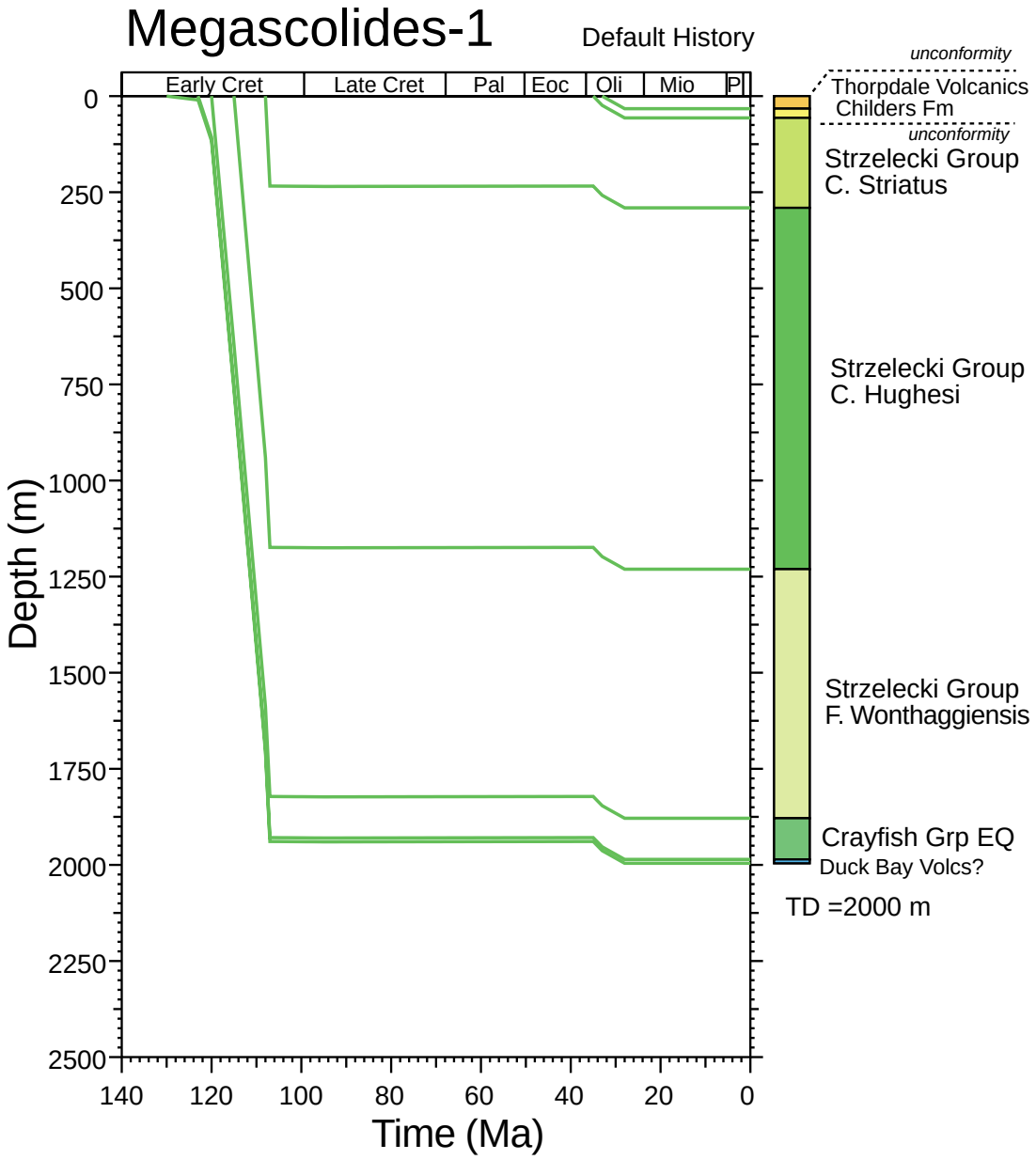

Figure 2.2: Default Burial History for the **Megascolides-1 well, Gippsland Basin**, derived from the preserved stratigraphy in the well. This burial history is combined with the present day present-day thermal gradient of 43.3°C/km (based on corrected BHT values - see Appendix A) to calculate the Default thermal history for estimation of the predicted VR profile shown in Figure 2.1.

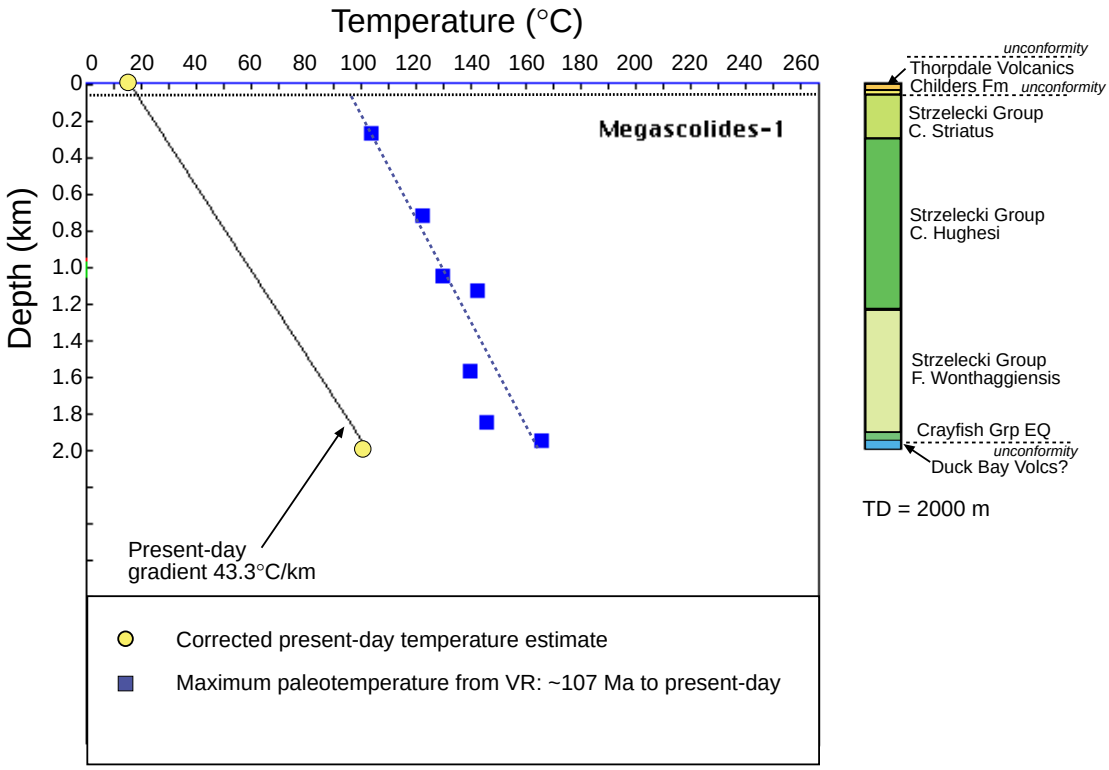

Figure 2.3: Paleotemperature constraints derived from VR data in the **Megascolides-1 well, Gippsland Basin**, plotted against depth. The estimated present-day temperature profile for this well based on geothermal gradient of 43.3°C/km and a surface temperature of 15°C is also shown (Appendix A).

A notional paleotemperature profile that honours the maximum paleotemperature estimates from VR is shown by the dashed line. Formal estimates of the paleogeothermal gradient are given in Figure 2.4

All paleotemperature estimates in this plot are summarised in Table i (Executive Summary).

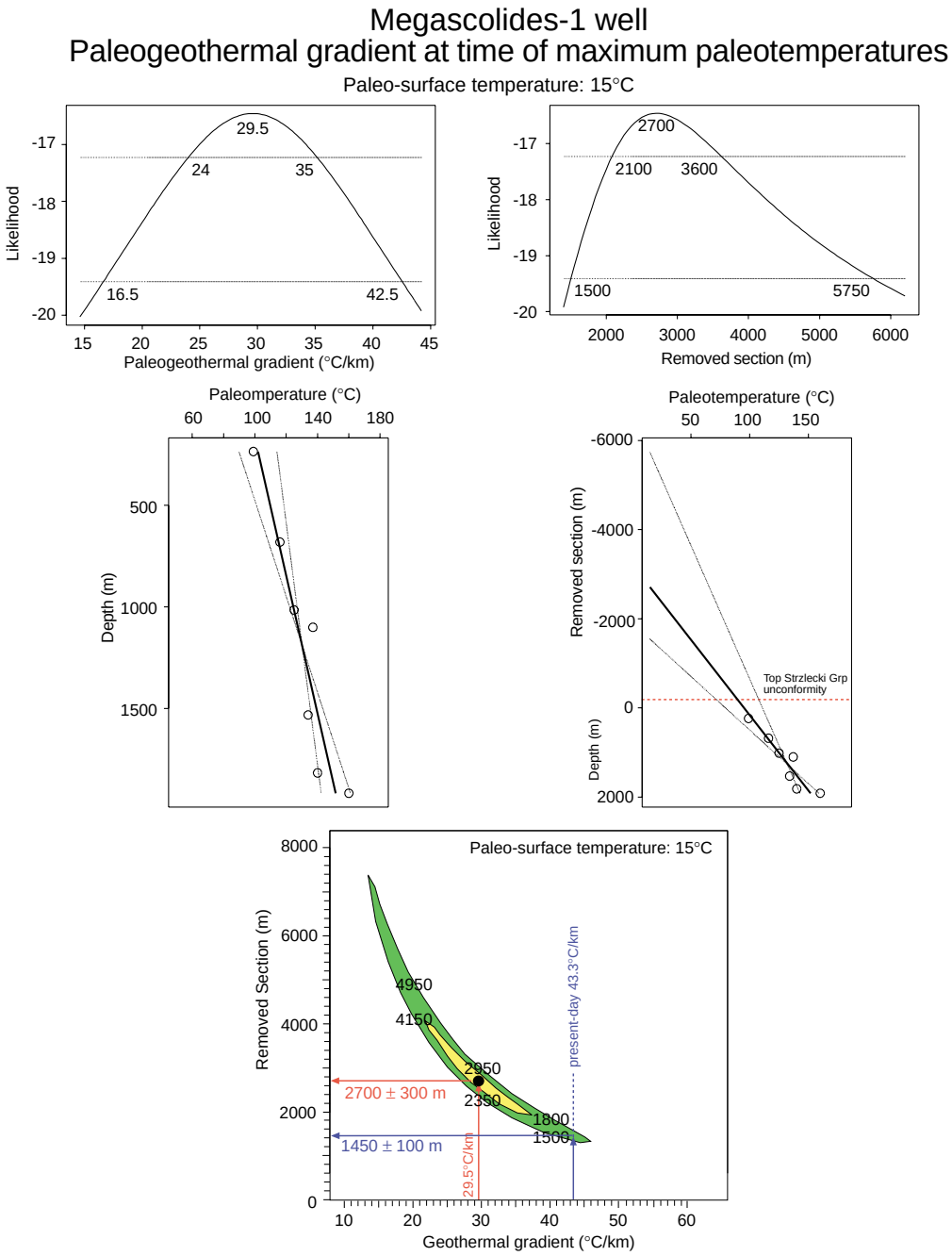

Figure 2.4: Paleogeothermal gradients & removed section estimates for the time of maximum paleotemperatures in Megascolides-1.

Upper: Maximum likelihood profiles of linear paleogeothermal gradient (left) and removed section (right) fitted to the **maximum paleotemperature** constraints from **all VR data** in this well. The methodology used to construct these profiles is outlined in Appendix C. In each plot, **maximum paleotemperature** constraints are plotted against depth below the top-Strzelecki Group unconformity at a depth of 61 m rKB in this well, also showing the best-fit profile (solid line) and lines (dashed) representing upper and lower 95% confidence limits. In the right-hand plot, the fitted gradients are extrapolated to a paleo-surface temperature of 15°C to determine removed section. Alternative paleo-surface temperatures can also be accomodated, as described in the text.
Lower: Crossplot of total section removed against paleogeothermal gradient, showing the ranges of paired values (within the contoured region) compatible with the **maximum paleotemperature** constraints at the 95% confidence level. Values printed within the plot are amounts of removed section corresponding to ±2σ limits at various values of paleogeothermal gradient. For example, for a paleogeothermal gradient of 43.3°C/km, equal to the present-day value, between 1350 and 1550 metres of additional burial is required on the top-Strzelecki Group unconformity in order to honour the paleotemperature constraints.

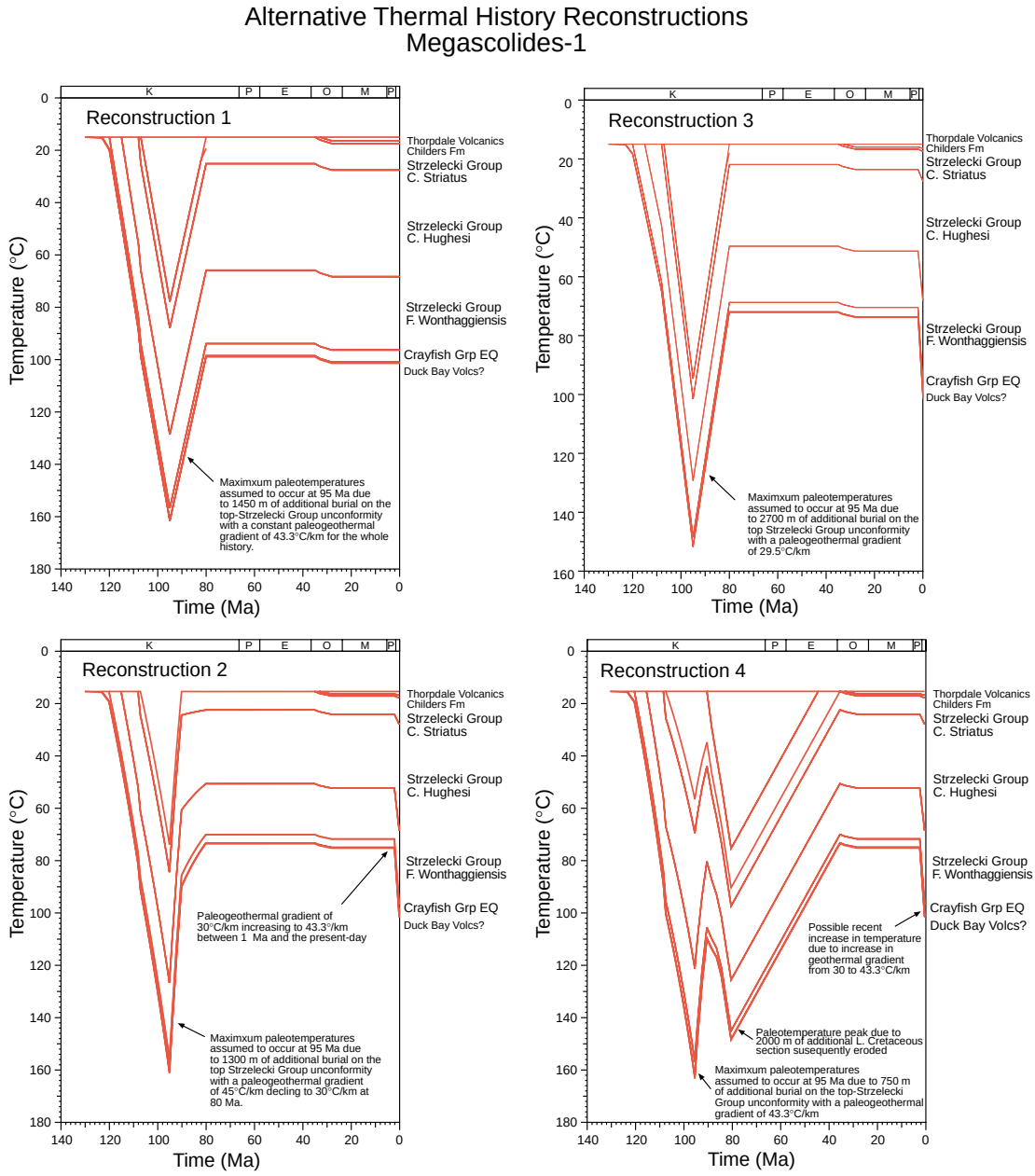

Figure 2.5: Some alternative thermal history reconstructions derived from interpretation of the VR data in the **Megascolides-1 well.**

Reconstruction 1: Geothermal gradient of 43.3°C/km for the whole history with 1450 m of additional Strzelecki Group section deposited between 107 and 95 Ma and eroded between 95 and 80 Ma.

Reconstruction 2: Geothermal gradient increasing from of 30°C/km at 135 Ma to 45°C/km at 95 Ma and declining to 30°C/km at 80 Ma, remaining at this level until 1 Ma then increasing to 43.3°C/km at the present day combined with 1300 m of additional Strzelecki Group section deposited between 107 and 95 Ma and eroded between 95 and 80 Ma.

Reconstruction 3: Geothermal gradient of 29.5°C/km from 135 Ma to 1 Ma increasing to 43.3°C/km at the present day. 2700 m of additional Strzelecki Group deposited between 107 & 95 Ma and eroded between 95 & 80 Ma.

Reconstruction 4: Geothermal gradient increasing from of 29.5°C/km at 135 Ma to 55°C/km at 95 Ma and declining to 29.5°C/km at 80 Ma, remaining at this level until 1 Ma then increasing to 43.3°C/km at the present day. This is combined with deposition of 750 m of additional Strzelecki Group section between 107 and 95 Ma, 250 m of which is eroded between 95 and 90 Ma, followed by deposition of 2000 m of Late Cretaceous section between 90 and 80 Ma with 2500 of section eroded between 80 and 35 Ma.

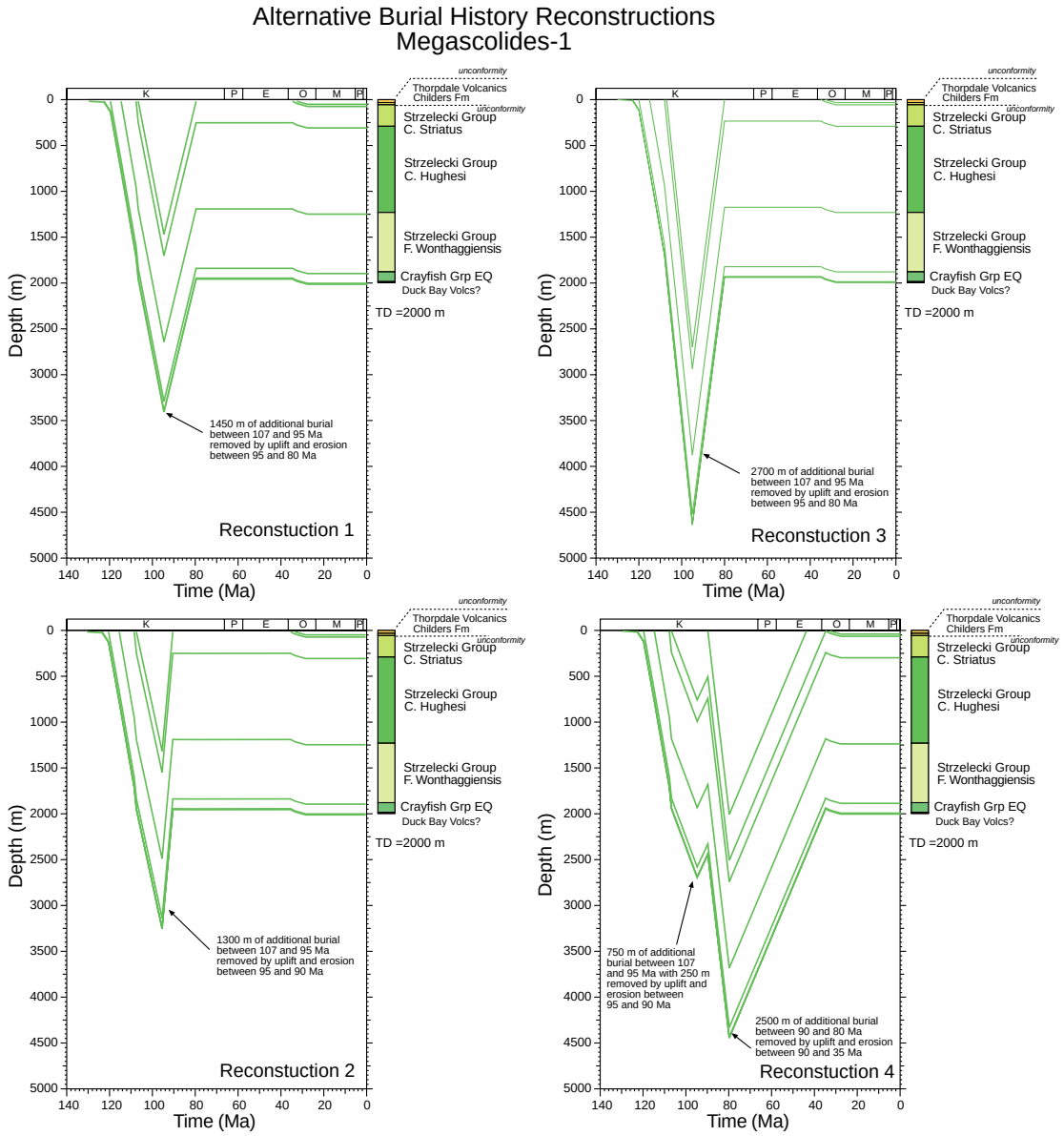

Figure 2.6: Alternative burial histories for the Megascolides-1 well matched with the alternative thermal history reconstructions shown in Figure 2.5

Reconstruction 1: 1450 m of additional Strzelecki Group section deposited between 107 and 95 Ma and eroded between 95 and 80 Ma.
Reconstruction 2: 1300 m of additional Strzelecki Group section deposited between 107 and 95 Ma and eroded between 95 and 90 Ma.
Reconstruction 3: 2700 m of additional Strzelecki Group section deposited between 107 and 95 Ma and eroded between 95 and 80 Ma.
Reconstruction 4: 750 m of additional Strzelecki Group section deposited between 107 and 95 Ma, 250 m of which is eroded between 95 and 90 Ma, followed by deposition of 2000 m of Late Cretaceous section between 90 and 80 Ma with 2500 of section eroded between 80 and 35 Ma.

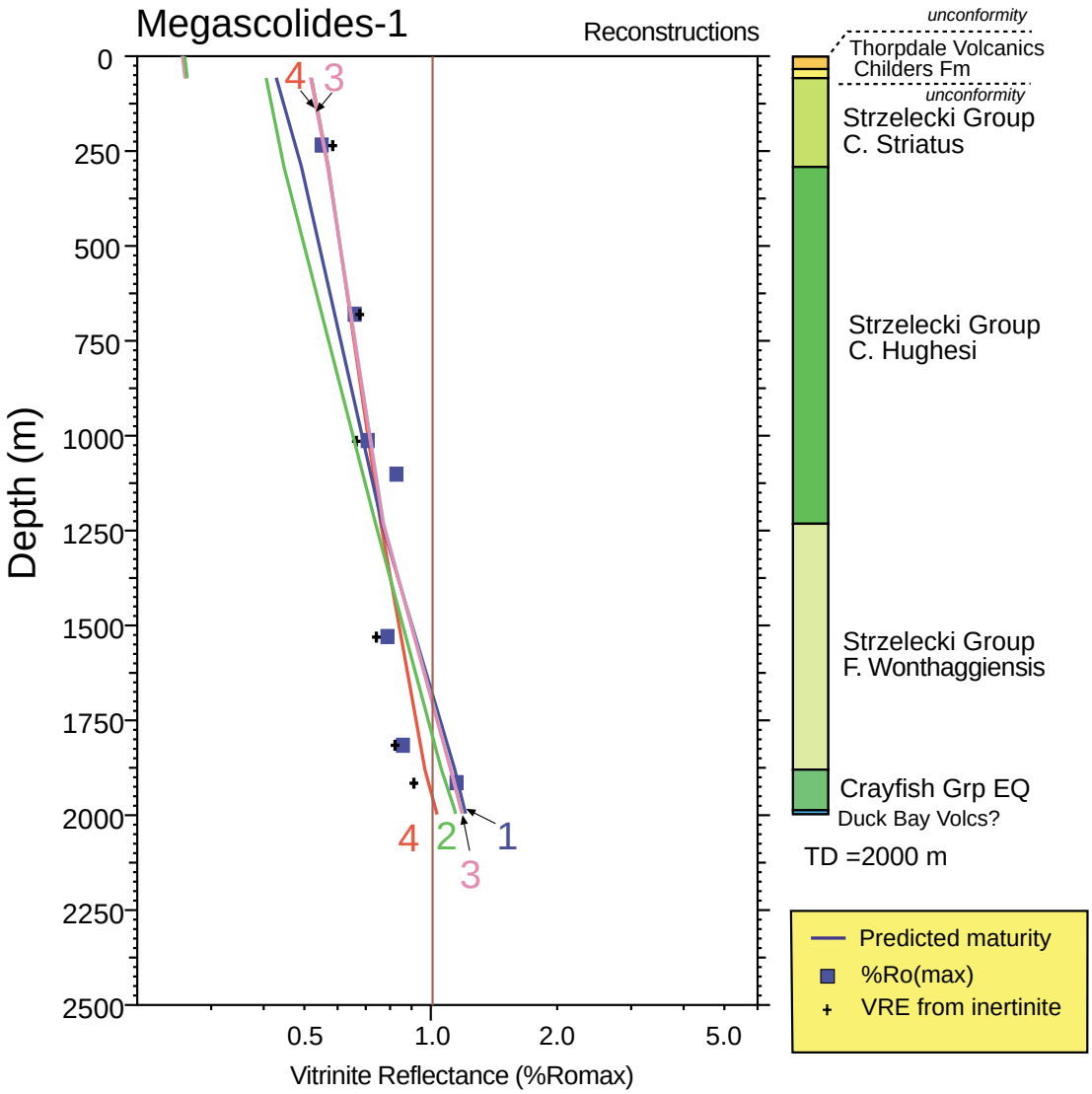

Figure 2.7: Mean vitrinite reflectance values (Table D.2, Appendix D) and VRE from inertinite in the **Megascolides-1 well** plotted against depth (TVD rkb), together with the three maturity profiles (numbered 1 to 4) predicted by the alternative Thermal Histories consistent with the VR data, as illustrated in Figure 2.5. All predicted profiles show an acceptable fit to the measured data. Application of AFTA to selected samples from this well is recommended in order to accurately quantify the thermal, burial and hydrocarbon source rock maturation histories at this location.

3 Concluding remarks: recommendations for additional work

The alternative thermal and burial histories for the Megascolides-1 well discussed in the previous section are all possible scenarios in terms of the measured VR data. Based on our regional knowledge, Reconstructions 2 and 4, or variations of these, are considered to be more geologically realistic, but without some direct information on the timing of heating, they should all be regarded as highly speculative. In particular, alternative histories with a more recent heating event at some time in the Tertiary have not been pursued, but are also possible on the basis of the available data.

We make the following recommendations for additional work would significantly enhance the understanding of the thermal evolution at this location:

1. In order to specifically address the question of the timing of heating a program of AFTA (apatite fission track analysis) is recommended from the Megascolides-1 well, with 5 samples taken from the Early Cretaceous Strzelecki and Crayfish groups. Application of AFTA will also enable direct assessment to be made of the duration of the present-day geothermal gradient of 43.3°C/km.

2. In addition, one or two additional VR samples from the Childers Fm clastic sequence is recommended in order to provide some simple constraints on the post-Oligocene thermal history that are currently available. The proposed AFTA sampling from the Early Cretaceous sequence will also provide direct constraints on the timing of any post-Oligocene heating should it be present.

3. Finally, some biostratigraphic determinations should also be attempted on the Childers Fm clastic sequence to establish the depositional age of this sequence.

References

Duddy, I.R., 1994 - The Otway Basin: Thermal, structural and tectonic and hydrocarbon generation Histories. in, Finlayson, D.M. (compiler), NGMA/PESA Otway Basin Symposium, Melbourne, 20 April 1994: extended abstracts, *Australian Geological Survey Organisation, Record 1999/14*, p.35-42.

Duddy, I.R., 1997 - Focussing exploration in the Otway Basin: Understanding timing of source rock maturation. *APPEA Journal*, **37**, 178-191.

Duddy, I.R. & Green, P.F. 1992: Tectonic Development of the Gippsland Basin and Environs: Identification of key episodes using Apatite Fission Track Analysis (AFTA®),*In* Energy, Economics and Environment, Gippsland Basin Symposium Melbourne 22-23 June, 111-120.

APPENDIX A

Sample Details, Geological Data and Apatite Compositions

A.1 Sample details

This report provides a discussion of possible thermal and burial histories reconstruction study of the **Megascolides-1 well, PEP-162, onshore Gippsland Basin** (Figure 1.1), based on vitrinite reflectance (VR) data. The study was commissioned by Mark Smith for **Karoon Gas Pty Ltd.**

No new vitrinite reflectance data were collected for this study but a suite of 7 VR determinations were supplied for the study by the client. Sample details and VR results are summarised in Table D.2 (Appendix D).

A.2 Stratigraphic details

Details of the stratigraphic breakdown of the preserved section in the **Megascolides-1 well** were provided by the client in the form of Formation tops together with a report on the palynology of the Early Cretaceous sequence. The chronostratic (relative succession) assignment of each sample was converted to a chronostratic (numerical) scale using Young and Laurie (1989), with the resulting information summarised in Table A.1.

The stratigraphic age of each VR sample, derived from this information, is summarised in Table D.2 (Appendix D).

Any slight errors in the estimated chronometric ages of each sample are not expected to affect the thermal history interpretation of the VR data to any significant degree.

A.3 Present temperatures

In application of any technique involving estimation of paleotemperatures, it is critical to control the present temperature profile, since estimation of maximum paleotemperatures proceeds from determining how much of the observed effect can be explained by the magnitude of present temperatures.

Recorded temperature data are often not reported in sufficient detail to allow rigorous analysis (typically consisting of single BHT measurements at a given depth for a single time

since circulation). A single measured BHT value was supplied by **Karoon Gas Pty Ltd** for the well and this was adjusted by a simplified correction procedure adapted from the literature (Oxburgh and Andrews-Speed, 1981; Andrews-Speed et al., 1984). While no doubt simplistic, this procedure has the advantage of allowing a common approach in all studies, and appears to give consistent results. Furthermore, the thermal history tools applied in this study are calibrated in studies using this same approach, and therefore use of this correction method provides a high degree of internal consistency.

Using a surface temperature of 15°C, quoted BHT data were corrected by increasing the difference between the surface temperature and the uncorrected BHT by 20% for uncorrected temperatures below 150°F (66°C), and by 25% above 150°F. Where multiple temperature measurements were available at a given depth, the earliest recorded BHT value is used. (Corrected BHT data derived from the above method are usually in good agreement with uncorrected DST data if these data are available). Where appropriate, a linear geothermal gradient, constrained to the surface temperature, is fitted to the BHT data corrected is this way.

The linear geothermal gradient estimated from the corrected temperature value is 43.3°C/km, constrained to a present-day surface temperature of 15°C as illustrated in Figure A.1. As only a single corrected temperature value is available, the quality of the geothermal gradient estimate cannot be assessed, but there is some evidence to suggest that it may be too high as discussed in Section 2 of the report.

References

Andrews-Speed, C.P., Oxburgh, E.R. and Cooper, B.A. (1984). Temperatures and depth-dependent heat flow in Western North Sea, *AAPG Bulletin*, 11, 1764 - 1784.

Oxburgh, E.R. and Andrews-Speed, C.P. (1981). Temperature, Thermal gradients and heat flow in the Southwestern North Sea. In: Illing, L. V. and Hobson, G.D. (eds.) The petroleum geology of the continental shelf of NW Europe, Heyden, 141 - 151.

Table A.1: Summary of stratigraphy - Megascolides-1, Gippsland Basin (Geotrack Report #938)

	KB elevation (mAMSL)	Ground level (m)	Stratigraphic Interval	Depth of Top TVD rKB (m)	Age of Top (Ma)
Megascolides-1					
	4.3	0	*Unconformity*	4.3	0
			Thorpdale volcs	4.3	25
			Unconformity	37	30
			Halibut sub-gp	37	33
			Unconformity	61	35
			Strezlecki C. striatus	61	107
			Strezlecki C. huglesi	295	108
			Strezlecki U.F. wonthaggiensis	1235	115
			Crayfish Gp	1883	120
			Unconformity	1942	123
			Duck Bay volcanics?	1942	130
			TD	2000	135

All depths quoted are with respect to KB, except where otherwise stated.

Table A.2: Summary of temperature data - Megascolides-1, Gippsland Basin (Geotrack Report #938)

KB elevation (mAMSL)	Ground level (m)	Depth (ft)	BHT (°F)	BHT (°C)	T.S.C (hrs)	Depth (m)	Corrected BHT (°C)	Geothermal gradient (°C/km)
Megascolides-1								
4.3	0							43.3
		6557	183.2	84.0	11.3	1998.5	101.3	

Quoted BHT values have been corrected by increasing the difference between surface temperature and measured BHT by 20% for measured temperatures <150°F (<66°C) and by 25% for temperatures >150°F (>66°C). A sea-bed temperature of 15°C has been assumed.

All depths quoted are with respect to KB, except where otherwise stated.

*Measurements not used in calculation of geothermal gradient.

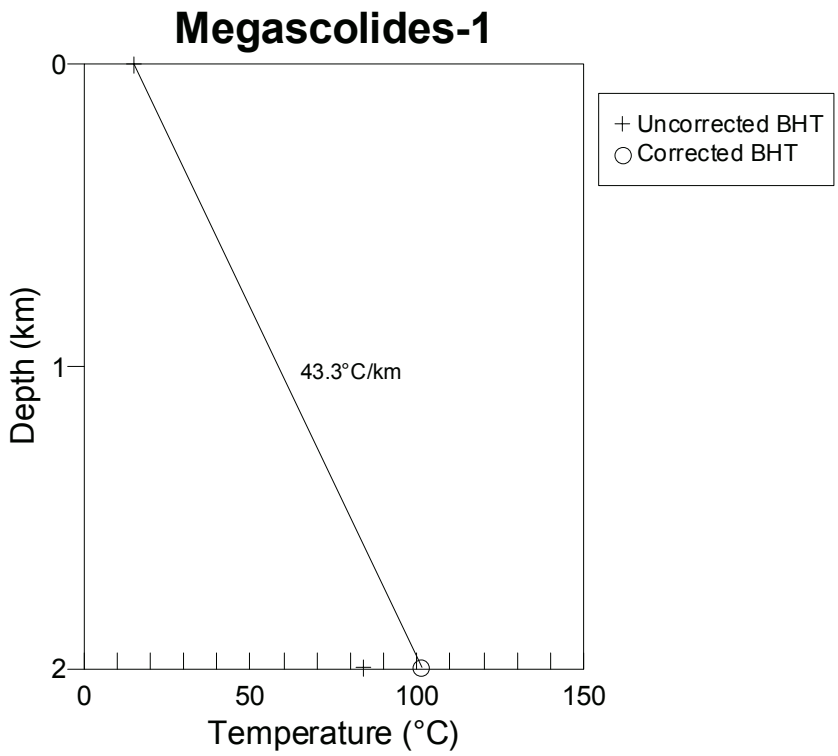

Figure A.1: Present temperature profile calculated for **well Megascolides-1, Gippsland Basin.** See Table A.4 and Appendix A for more detail.

APPENDIX B: Thermal History Interpretation Strategy

B.1 Thermal history interpretation of VR data

Basic principles

Interpretation of VR data in this report begins by assessing whether the measured VR value in each sample could have been produced if the sample has never been hotter than its present temperature at any time since deposition. To this end, we consider a "Default Thermal History" for each sample, which forms the basis of interpretation. Default Thermal Histories throughout a well are derived from the stratigraphy of the preserved sedimentary section, combined with constant values for paleogeothermal gradient and paleo-surface temperature which are adopted from present-day values. For outcrop samples, the Default Thermal Histories simply represent long-term residence at the prevailing surface temperature.

If a measured VR value is higher than the value predicted from the Default Thermal History (making due allowance for analytical uncertainty), the sample must have been hotter at some time in the past. In this case, VR data provide an independent estimate of maximum paleotemperature, which can be calculated using an assumed heating rate and timing information provided from AFTA data, if available (assumed, otherwise). Cooling rates do not significantly affect VR data, which are dominated by the maximum paleotemperature provided that cooling occurs immediately after reaching the thermal maximum. If both AFTA and VR data are available from the same sample or well, then an identical heating rate must be used to obtain consistent paleotemperature estimates.

If a measured VR value is lower than expected on the basis of the Default Thermal History, either present temperatures may have been overestimated or temperatures have increased very recently. In such cases, the measured VR value may allow an estimate of the true present-day temperature. Alternatively the measured VR value may underestimate the true maturity for some other reason, e.g., suppression of reflectance in certain organic macerals, misidentification of true "in-situ" vitrinite, presence of caved material etc. Comparison of AFTA and VR data usually allows such factors to be identified, and where applicable they are discussed in the relevant section of text.

Vitrinite reflectance data (specifically $R_o$max values) are predicted using the distributed activation energy model describing the evolution of VR, with temperature and time developed by Burnham and Sweeney (1989) (see also Sweeney and Burnham, 1990).

Values of VR less than ~0.3% and greater than 5% cannot be assigned to a specific maximum paleotemperature with confidence, and such values are given maximum and minimum limits, respectively, appropriate to the particular heating rate used (see Appendix D). Further discussion of the methodology employed in interpreting VR data are given in Appendix D, which also briefly discusses the benefits of integrating AFTA and VR data.

Specific to this report

For this report, VR data in all samples have been interpreted using a heating rate of 5°C/Ma and a cooling rate of 10°C/Ma.

Maximum paleotemperatures determined for the VR samples are generally attributed to one of the paleo-thermal episodes identified by AFTA on the basis of comparison of the VR-derived maximum paleotemperature with observed paleo-heating of a similar style in adjacent AFTA samples. In this study no AFTA data are available and the VR data are simply referred to the "Maximum Paleotemperature Event", the timing of which is speculated upon in Section 2 of this report.

B.2 Comparison of paleotemperature estimates from AFTA and VR

Maximum paleotemperatures derived from AFTA and VR ($R_o$max) using the strategies outlined above are usually highly consistent. Estimates of maximum paleotemperature from VR (Table i) are usually quoted to the nearest degree Celsius, as the value which predicts the exact measured reflectance. This is not meant to imply VR data can be used to estimate paleotemperatures to this degree of precision. VR data from individual samples typically show a scatter equivalent to a range of between ±5 and ±10°C. Estimates from a series of samples are normally used to define a paleotemperature profile in samples from a well, or a regional trend in paleotemperatures from outcrop samples.

B.3 Estimates of paleogeothermal gradients and mechanisms of heating and cooling

Basic principles

A series of paleotemperature estimates from AFTA and/or VR over a range of depths can be used to reconstruct a paleotemperature profile through the preserved section. The slope of this profile defines the paleogeothermal gradient. As explained by Bray et al. (1992), the shape of the paleotemperature profile and the magnitude of the

paleogeothermal gradient provides unique insights into the origin and nature of the heating and cooling episodes expressed in the observed paleotemperatures (Figure B.1).

Linear paleotemperature profiles with paleogeothermal gradients close to the present-day geothermal gradient provide strong evidence that heating was caused by greater depth of burial with no significant increase in basal heat flow, implying in turn that cooling was due to uplift and erosion. Paleogeothermal gradients significantly higher than the present-day geothermal gradient suggest that heating was due, at least in part, to increased basal heat flow, while a component of deeper burial may also be important as discussed in the next section. Paleogeothermal gradients significantly lower than the present-day geothermal gradient suggest that a simple conductive model is inappropriate, and more complex mechanisms must be sought for the observed heating. One common cause of low paleogeothermal gradients is transport of hot fluids shallow in the section (Figure B.1). However the presence of large thicknesses of sediment with uniform lithology dominated by high thermal conductivities can produce similar paleotemperature profiles and each case has to be considered individually.

A paleotemperature profile can only be characterised by a single value of paleogeothermal gradient when the profile is linear. Departures from linearity may occur where strong contrasts in thermal conductivities occur within the section, or where hot fluid movement or intrusive bodies have produced localised heating effects. In such cases a single value of paleogeothermal gradient cannot be calculated, and different values (possibly negative) may apply through different parts of the section. However it is important to recognise that the validity of the paleotemperatures determined from AFTA and/or VR are independent of these considerations, and can still be used to control possible thermal history models.

Estimation of paleogeothermal gradients in this report

In this report, a paleogeothermal gradient has been estimated for the “Maximum Paleotemperature Event” based on paleotemperature estimates from the VR data over a range of depths using methods outlined in Appendix C. These methods provide a best estimate of the gradient (“maximum likelihood value”) and upper and lower 95% confidence limits on this estimate (analogous to ±2s limits). The “goodness of fit” is displayed in the form of a log-likelihood profile, which is expected to show good quadratic behaviour for a dataset which agrees with a linear profile. This analysis depends on the assumption that the paleogeothermal gradient through the preserved section is linear. Visual inspection is usually sufficient to confirm or reject this assumption.

B.4 Determination of removed section

Basic principles

Subject to a number of important assumptions, extrapolation of a linear paleotemperature profile to a paleo-surface temperature allows estimation of the amount of eroded section represented by an unconformity, as explained in more detail in Section C.9 (Appendix C).

Specifically, this analysis assumes:

- The paleotemperature profile through the preserved section is linear
- The paleogeothermal gradient through the preserved section can be extrapolated linearly through the missing section.
- The paleo-surface (or sea-bed) temperature is known.
- The heating rate used to estimate the paleotemperatures defining the paleogeothermal gradient is correct

It is important to realise that any method of determining the amount of eroded section based on thermal methods is subject to these and/or additional assumptions. For example methods based on heat-flow modelling must assume values of thermal conductivities in the eroded section, which can never be known with confidence. Such models also require some initial assumption of the amount of eroded section to allow for the effect of compaction on thermal conductivity. Methods based on geothermal gradients, as used in this study, are unaffected by this consideration, and can therefore provide independent estimates of the amount of eroded section. But these estimates are always subject to the assumptions set out above, and should be considered with this in mind.

The analysis used to estimate paleogeothermal gradients is easily extended to provide maximum likelihood values of eroded section for an assumed paleo-surface temperature, together with ±95% confidence limits. These parameters are quoted for each well in which the paleotemperature profile suggests that heating may have been due, at least in part, to deeper burial.

Estimates of paleogeothermal gradient and eroded section derived from fitting linear profiles to paleotemperature data as a function of depth are highly correlated, since the profile is constrained to pass through the main body of the data. Thus, higher paleo-gradients within the allowed range correspond to lower amounts of section removed, while lower paleo-gradients correspond to higher amounts of removed

section. In plots of paleogeothermal gradient against removed section, paired values of each parameter which are consistent with the paleotemperature data can be defined, thus allowing the range of allowed values at various levels of statistical significance to be contoured. In general, the greater the depth interval over which paleotemperature constraints are available, the tighter the resulting constraints on both the paleogeothermal gradient and the amount of removed section.

However, it is emphasised that reconstructed burial histories produced in this way do not produce unique solutions, and alternative interpretations are always possible. For instance, where the eroded section was dominated by units with high thermal conductivities the paleogeothermal gradient through the missing section may have been much higher than in the preserved section, and extrapolation of a linear gradient will lead to overestimation of the eroded section.

Specific to this report

For the samples analysed in this report, any estimates of eroded section are conditional on:

- Heating rates of 5°C/Ma and cooling rates of 10°C/Ma in each episode, and
- An assumed value of paleo-surface temperature of 15°C,

as well as the other assumptions outlined above.

The effects of higher paleo-surface temperatures can be simply allowed for by subtracting the depth increment corresponding to the increase in temperature, for the appropriate value of paleogeothermal gradient. For instance, if the paleogeothermal gradient was 30°C/km and the paleo-surface temperature was *10°C higher* than the value assumed in this report, the estimated eroded section should be *reduced by 333 metres*. Different heating rates can be allowed for in similar fashion, with an order of magnitude change in heating rate equivalent to a 10°C change in paleotemperature (paleotemperatures increase for higher heating rates, and decrease for lower heating rates). For typical values, the assumed value of heating rate will not affect the shape or slope of the paleotemperature profile significantly.

Multiple exhumation episodes

In the previous discussion, it is important to emphasise that estimates of removed section derived in this way represent the total amount of sediment removed since the onset of cooling (i.e. exhumation) from the maximum (or peak) paleotemperatures from which the estimates were derived. In this sense, these estimates can be thought of as representing “paleo-burial”, i.e. the amount by which the preserved section (in

which the paleotemperatures were recorded) was more deeply buried, prior to the onset of the exhumation episode.

In the case of a single cooling episode, in which the additional section was fully removed prior to the onset of deposition of sediment which has been preserved to the present day, such estimates of paleo-burial are identical to the amount of removed section in that episode. In such cases, it is clear that the unconformity surface, on which the additional section was deposited, returned to the surface before the re-commencement of deposition. However, where multiple exhumation episodes occur within a relatively long interval for which no sediments are preserved, this is not necessarily true. In this case, there is no evidence to demonstrate whether the unconformity surface at the top of the now preserved section returned entirely to the surface following an initial exhumational episode (i.e. if the entire amount of additional sediment was eroded), or if only part of the additional section was eroded prior to the re-commencement of deposition (after which a later exhumation episode resulted in removal of all the additional section). This situation is summarised in Figure B.2, in the context of an outcrop sample, although similar principles apply to well samples.

In the notional example shown in Figure B.2, two cooling episodes are identified by AFTA (grey zones) within a time interval represented by a single unconformity. The sampled unit cooled from its maximum paleotemperature in the Early Tertiary, and subsequently cooled from a lower paleotemperature peak in the Late Tertiary. Since AFTA only records the maximum or peak paleotemperatures in each event, which provide the estimates of paleo-burial for those episodes, no information on the approach to those paleotemperatures is preserved. For this reason, although the amount of section removed in the Late Tertiary episode, E_2, is well constrained, the amount of additional section deposited in that episode, D_2, is not. Conversely, while the total amount of section removed since the onset of Early Tertiary cooling (i.e. the Early Tertiary paleo-burial), D_1, is well constrained, the amount of section removed by erosion in the earlier exhumation episode (E_1) is not well constrained. Only for the case where the unit returned to the surface (red path) before burial re-commenced, are D_1 and E_1 equal, and E_1 is well constrained. But if sediments laid down in the mid-Tertiary are not preserved to the present-day, then no record of this return to the surface is available, and therefore the absolute magnitude of E_1 is not clear. Similar considerations apply to well samples, except that the present-day depth should be substituted for the surface.

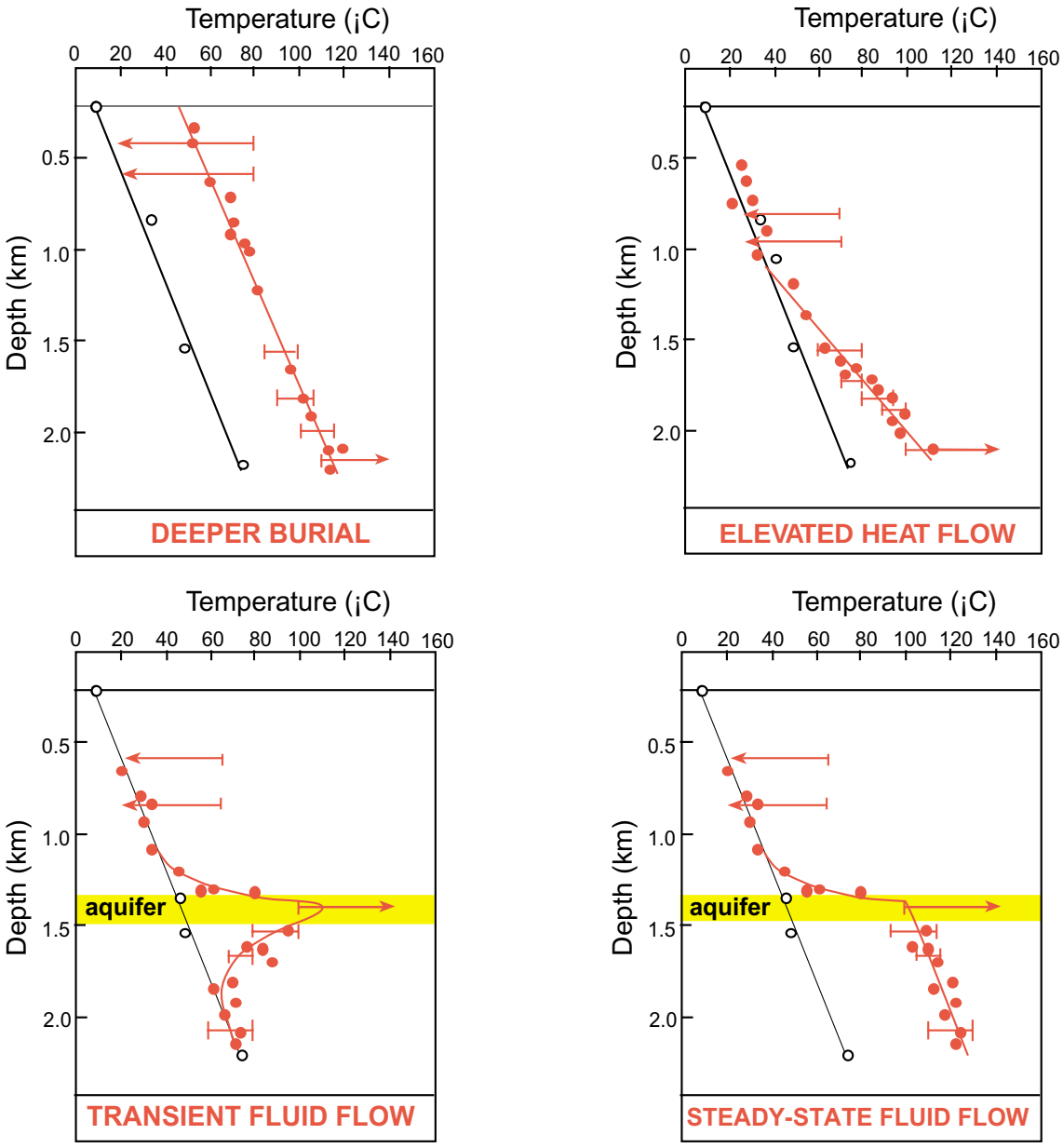

Figure B.1: The way in which paleotemperatures characterising a particular paleo-thermal episode vary with depth, or the "paleotemperature profile", provides key information on the mechanisms of heating and cooling. See text for details.

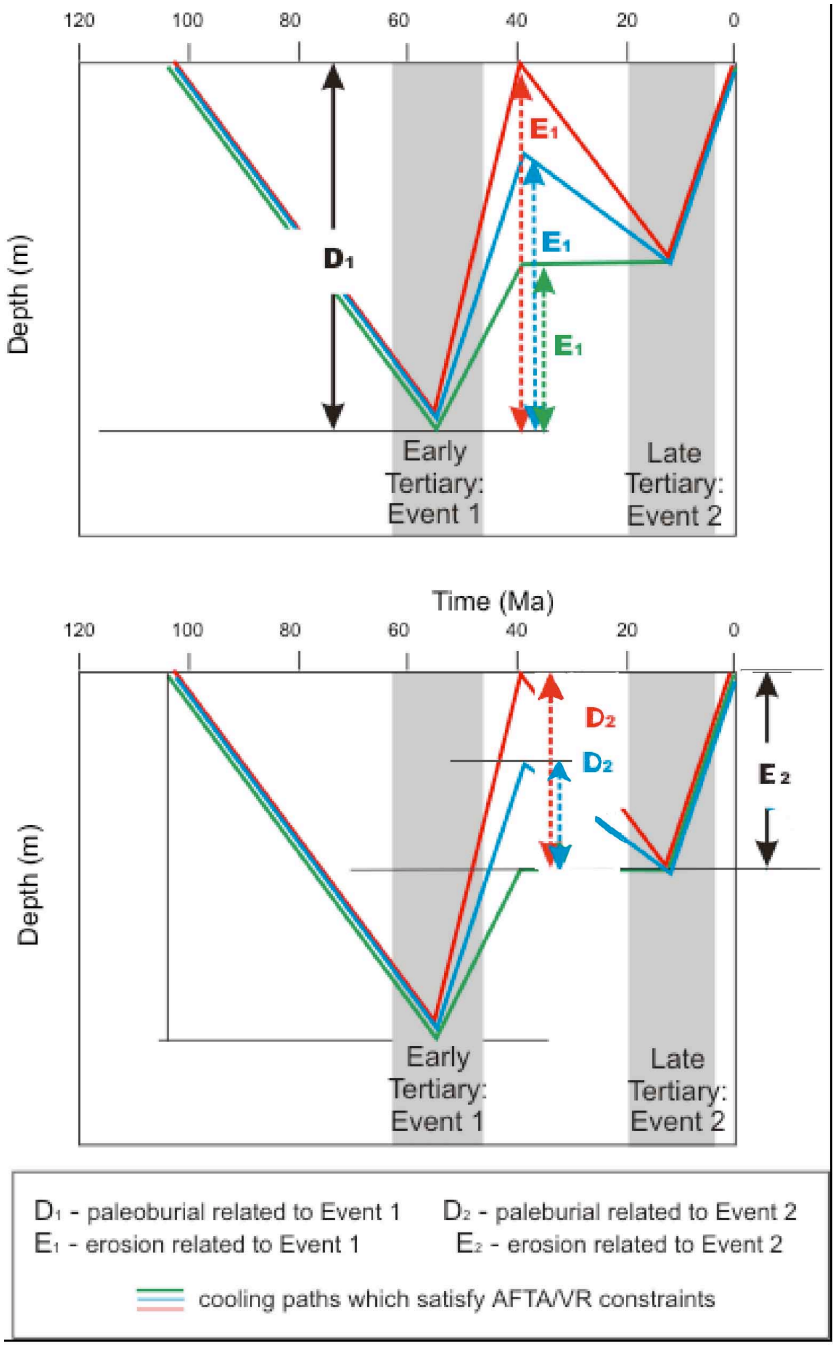

Figure B.2: Where multiple exhumation episodes occur within an interval represented by a single unconformity, it is not possible to determine the total amount of section removed during the earlier exhumation episode, only the total amount removed since the onset of cooling in that episode and the present day. In this example, E_2 is uniquely defined by the total section removed during the later episode, while D_1 is uniquely defined by the total amount of additional burial required to explain the paleotemperatures in the earlier episode. But E_1 and D_2 and not uniquely defined (see text for detailed explanation).

APPENDIX C

Principles of Interpretation of AFTA Data in Sedimentary Basins

C.1 Introduction

Detrital apatite grains are incorporated into sedimentary rocks from three dominant sources - crystalline basement rocks, older sediments and contemporaneous volcanism. Apatites derived from the first two sources will, in general, contain fission tracks when they are deposited, with AFTA parameters characteristic of the source regions. However, apatites derived from contemporaneous volcanism, or from rapidly uplifted basement, will contain no tracks when they are deposited. For now, we will restrict discussion to this situation, and generalise at a later point to cover the case of apatites which contain tracks that have been inherited from source regions.

C.2 Basic principles of Apatite Fission Track Analysis

Fission tracks are trails of radiation damage, which are produced within apatite grains at a more or less constant rate through geological time, as a result of the spontaneous fission of ^{238}U impurity atoms. Therefore, the number of fission events which occur within an apatite grain during a fixed time interval depends on the magnitude of the time interval and the uranium content of the grain. Each fission event leads to the formation of a single fission track, and the proportion of tracks which can intersect a polished surface of an apatite grain depends on the length of the tracks. Therefore, the number of tracks which are etched in unit area of the surface of an apatite grain (the "spontaneous track density") depends on three factors - (i) The time over which tracks have been accumulating; (ii) The uranium content of the apatite grain; and, (iii) The distribution of track lengths in the grain. In sedimentary rocks which have not been subjected to temperatures greater than ~50°C since deposition, spontaneous fission tracks have a characteristic distribution of confined track lengths, with a mean length in the range 14-15 µm and a standard deviation of ~1 µm. In such samples, by measuring the spontaneous track density and the uranium content of a collection of apatite grains, a "fission track age" can be calculated which will be equal to the time over which tracks have been accumulating. The technique is calibrated against other isotopic systems using age standards which also have this type of length distribution (see Appendix B).

In samples which have been subjected to temperatures greater than ~50°C after deposition, fission tracks are shortened because of the gradual repair of the radiation damage which constitutes the unetched tracks. In effect, the tracks shrink from each end, in a process which is known as fission track "annealing". The final length of each individual track is essentially determined by the maximum temperature which that track has experienced. A time difference of an order of magnitude produces a change in fission track parameters which is equivalent to a temperature change of only ~10°C, so temperature is by far the dominant factor in determining the final fission track parameters. As temperature increases, all existing tracks shorten to a length determined by the prevailing temperature, regardless of when they were formed. After the temperature has subsequently decreased, all tracks formed prior to the thermal maximum are "frozen" at the degree of length reduction they attained at that time. Thus, the length of each track can be thought of as a maximum-reading thermometer, recording the maximum temperature to which it has been subjected.

Therefore, in samples for which the present temperature is maximum, all tracks have much the same length, resulting in a narrow, symmetric distribution. The degree of shortening will depend on the temperature, with the mean track length falling progressively from ~14 µm at 50°C, to zero at around 110°-120°C - the precise temperature depending on the timescale of heating and the composition of the apatites present in the sample (see below). Values quoted here relate to times of the order of 10^7 years (heating rates around 1 to 10°C/Ma) and average apatite composition. If the effective timescale of heating is shorter than 10^7 years, the temperature responsible for a given degree of track shortening will be higher, depending in detail on the kinetics of the annealing process (Green et al., 1986; Laslett et al., 1987; Duddy et al., 1988; Green et al., 1989b). Shortening of tracks produces an accompanying reduction in the fission track age, because of the reduced proportion of tracks which can intersect the polished surface. Therefore, the fission track age is also highly temperature dependent, falling to zero at around 120°C due to total erasure of all tracks.

Samples which have been heated to a maximum paleotemperature less than ~120°C at some time in the past and subsequently cooled will contain two populations of tracks, and will show a more complex distribution of lengths and ages. If the maximum paleotemperature was less than ~50°C then the two components will not be resolvable, but for maximum paleotemperatures between ~50° and 120°C the presence of two components can readily be identified. Tracks formed prior to the thermal maximum will all be shortened to approximately the same degree (the precise value depending on the maximum paleotemperature), while those formed during and after cooling will be longer, due to the lower prevailing temperatures. The length distribution in such

samples will be broader than in the simple case, consisting of a shorter and a longer component, and the fission track age will reflect the amount of length reduction shown by the shorter component (determined by the maximum paleotemperature).

If the maximum paleotemperature was sufficient to shorten tracks to between 9 and 11 µm, and cooling to temperatures of ~50°C or less was sufficiently rapid, tracks formed after cooling will have lengths of 14-15 µm and the resulting track length distribution will show a characteristic bimodal form. If the maximum paleotemperature was greater than ~110 to 120°C, all pre-existing tracks will be erased, and all tracks now present will have formed after the onset of cooling. The fission track age in such samples relates directly to the time of cooling.

In thermal history scenarios in which a heating episode is followed by cooling and then temperature increases again, the tracks formed during the second heating phase will undergo progressive shortening. The tracks formed prior to the initial cooling, which were shortened in the first heating episode, will not undergo further shortening until the temperature exceeds the maximum temperature reached in the earlier heating episode. (In practice, differences in timescale of heating can complicate this simple description. In detail, it is the integrated time-temperature effect of the two heating episodes which should be considered.) If the maximum and peak paleotemperatures in the two episodes are sufficiently different (>~10°C), and the later peak paleotemperature is less than the earlier maximum value, then the AFTA parameters allow determination of both episodes. As the peak paleotemperature in the later episode approaches the earlier maximum, the two generations of tracks become increasingly more difficult to resolve, and when the two paleotemperatures are the same, both components are shortened to an identical degree and all information on the earlier heating phase will be lost.

No information is preserved on the approach to maximum paleotemperature because the great majority of tracks formed up to that time have the same mean track length. Only those tracks formed in the last few per cent of the history prior to the onset of cooling are not shortened to the same degree (because temperature dominates over time in the annealing kinetics). These form a very small proportion of the total number of tracks and therefore cannot be resolved within the length distribution because of the inherent spread of several µm in the length distribution.

To summarise, AFTA allows determination of the magnitude of the maximum temperature and the time at which cooling from that maximum began. In some circumstances, determination of a subsequent peak paleotemperature and the time of cooling is also possible.

C.3 Quantitative understanding of fission track annealing in apatite

Annealing kinetics and modelling the development of AFTA parameters

Our understanding of the behaviour of fission tracks in apatite during geological thermal histories is based on study of the response of fission tracks to elevated temperatures in the laboratory (Green et al., 1986; Laslett et al., 1987; Duddy et al., 1988; Green et al., 1989b), in geological situations (Green et al., 1989a), observations of the lengths of spontaneous tracks in apatites from a wide variety of geological environments (Gleadow et al., 1986), and the relationship between track length reduction and reduction in fission track age observed in controlled laboratory experiments (Green, 1988).

These studies resulted in the capability to simulate the development of AFTA parameters resulting from geological thermal histories for an apatite of average composition (Durango apatite, ~0.43 wt% Cl). Full details of this modelling procedure have been explained in Green et al. (1989b). The following discussion presents a brief explanation of the approach.

Geological thermal histories involving temperatures varying through time are broken down into a series of isothermal steps. The progressive shortening of track length through sequential intervals is calculated using the extrapolated predictions of an empirical kinetic model fitted to laboratory annealing data. Contributions from tracks generated throughout the history (remembering that new tracks are continuously generated through time as new fissions occur) are summed to produce the final distribution of track lengths expected to result from the input history. In summing these components, care is taken to allow for various biases which affect revelation of confined tracks (Laslett et al., 1982). The final length reduction of each component of tracks is converted to a contribution of fission track age, using the relationship between track length and density reduction determined by Green (1988). These age contributions are summed to generate the final predicted fission track age.

This approach depends critically on the assumption that extrapolation of the laboratory-based kinetic model to geological timescales, over many orders of magnitude in time, is valid. This was assessed critically by Green et al. (1989b), who showed that predictions from this approach agree well with observed AFTA parameters in apatites of the appropriate composition in samples from a series of reference wells in the Otway Basin of south-east Australia (Gleadow and Duddy, 1981; Gleadow et al., 1983; Green et al., 1989a). This point is illustrated in Figure C.1. Green et al. (1989b) also quantitatively assessed the errors associated with extrapolation of the Laslett et al. (1987) model from

laboratory to geological timescales (i.e. precision, as opposed to accuracy). Typical levels of precision are ~0.5 µm for mean lengths <~10 µm, and ~0.3 µm for lengths >~10 µm. These figures are equivalent to an uncertainty in estimates of maximum paleotemperature derived using this approach of ~10°C. Precision is largely independent of thermal history for any reasonable geological history. Accuracy of prediction from this model is limited principally by the effect of apatite composition on annealing kinetics, as explained in the next section.

Compositional effects

Natural apatites essentially have the composition $Ca_5(PO_4)_3(F,OH,Cl)$. Most common detrital and accessory apatites are predominantly Fluor-apatites, but may contain appreciable amounts of chlorine. The amount of chlorine in the apatite lattice exerts a subtle compositional control on the degree of annealing, with apatites richer in fluorine being more easily annealed than those richer in chlorine. The result of this effect is that in a single sample, individual apatite grains may show a spread in the degree of annealing (i.e. length reduction and fission track age reduction). This effect becomes most pronounced in the temperature range 90 - 120°C (assuming a heating timescale of ~10 Ma), and can be useful in identifying samples exposed to paleotemperatures in this range. At temperatures below ~80°C, the difference in annealing sensitivity is less marked, and compositional effects can largely be ignored.

Our original quantitative understanding of the kinetics of fission track annealing, as described above, relates to a single apatite (Durango apatite) with ~0.43 wt% Cl, on which most of our original experimental studies were carried out. Recently, we have extended this quantitative understanding to apatites with Cl contents up to ~3 wt%. This new, multi-compositional kinetic model is based both on new laboratory annealing studies on a range of apatites with different F-Cl compositions (Figure C.2), and on observations of geological annealing in apatites from a series of samples from exploration wells in which the section is currently at maximum temperature since deposition. A composite model for Durango apatite composition was first created by fitting a common model to the old laboratory data (from Green et al., 1986) and the new geological data for a similar composition. This was then extended to other compositions on the basis of the multi-compositional laboratory and geological data sets. Details of the multi-compositional model are contained in a Technical Note, available from Geotrack in Melbourne.

The multi-compositional model allows prediction of AFTA parameters for any Cl content between 0 and 3 wt%, using a similar approach to that used in our original single composition modelling, as outlined above. Then, for an assumed or measured distribution of Cl contents within a sample, the composite parameters for the sample can be predicted. The range of Cl contents from 0 to 3 wt% spans the range of compositions commonly encountered, as discussed in the next section.

Predictions of the new multi-compositional model are in good agreement with the geological constraints on annealing rates provided by the Otway Basin reference wells, as shown in Figure C.3. However, note that the AFTA data from these Otway Basin wells were among those used in construction of the new model, so this should not be viewed as independent verification, but rather as a demonstration of the overall consistency of the model.

Distributions of Cl content in common AFTA samples

Figure C.4a shows a histogram of Cl contents, measured by electron microprobe, in apatite grains from more than 100 samples of various types. Most grains have Cl contents less than ~0.5 wt%. The majority of grains with Cl contents greater than this come from volcanic sources and basic intrusives, and contain up to ~2 wt% Cl. Figure C.4b shows the distribution of Cl contents measured in randomly selected apatite grains from 61 samples of "typical" quartzo-feldspathic sandstone. This distribution is similar to that in Figure C.4a, except for a more rapid fall-off as Cl content increases. Apatites from most common sandstones give distributions of Cl content which are very similar to that in Figure C.4b. Volcanogenic sandstones typically contain apatites with higher Cl contents, with a much flatter distribution for Cl contents up to ~1.5%, falling to zero at ~2.5 to 3 wt%, as shown in Figure C.4c. Cl contents in granitic basement samples and high-level intrusives are typically much more dominated by compositions close to end-member Fluorapatite, although many exceptions occur to this general rule.

Information about the spread of Cl contents in samples analysed in this report can be found in Appendix A.

Alternative kinetic models

Recently, both Carlson (1990) and Crowley et al. (1991) have published alternative kinetic models for fission track annealing in apatite. Carlson's model is based on our laboratory annealing data for Durango apatite (Green et al., 1986) and other (unpublished) data. In his abstract, Carlson claims that because his model is "based on explicit physical mechanisms, extrapolations of annealing rates to the lower temperatures and longer timescales required for the interpretation of natural fission track

length distributions can be made with greater confidence than is the case for purely empirical relationships fitted to the experimental annealing data". As explained in detail by Green et al. (1993), all aspects of Carlson's model are in fact purely empirical, and his model is inherently no "better" for the interpretation of data than any other. In fact, detailed inspection shows that Carlson's model does not fit the laboratory data set at all well. Therefore, we recommend against use of this model to interpret AFTA data.

The approach taken by Crowley et al. (1991) is very similar to that taken by Laslett et al., (1987). They have fitted models to new annealing data in two apatites of different composition - one close to end-member Fluorapatite (B-5) and one having a relatively high Sr content (113855). The model developed by Crowley et al. (1991) from their own annealing data for the B-5 apatite gives predictions in geological conditions which are consistently higher than measured values, as shown in Figure C.5. Corrigan (1992) reported a similar observation in volcanogenic apatites in samples from a series of West Texas wells. Since the B-5 apatite is close to end-member Fluor-apatite, while the Otway Group apatites contain apatites with Cl contents from zero up to ~3 wt% (and the West Texas apatites have up to 1 wt%), the fluorapatites should have mean lengths rather less than the measured values, which should represent a mean over the range of Cl contents present. Therefore, the predictions of the Crowley et al. (1991) B-5 model appear to be consistently high.

We attribute this to the rather restricted temperature-time conditions covered by the experiments of Crowley et al. (1991), with annealing times between one and 1000 hours, in contrast to times between 20 minutes and 500 days in the experiments of Green et al. (1986). In addition, few of the measured length values in Crowley et al.'s study fall below 11 μm (in only five out of 60 runs in which lengths were measured in apatite B-5) and their model is particularly poorly defined in this region.

Crowley et al. (1991) also fitted a new model to the annealing data for Durango apatite published by Green et al. (1986). Predictions of their fit to our data are not very much different to those from the Laslett et al. (1987) model (Figure C.6). We have not pursued the differences between their model and ours in detail because the advent of our multi-compositional model has rendered the single compositional approach obsolete.

C.4 Evidence for elevated paleotemperatures from AFTA

The basic principle involved in the interpretation of AFTA data in sedimentary basins is to determine whether the degree of annealing shown by tracks in apatite from a particular sample could have been produced if the sample has never been hotter than its present temperature at any time since deposition. To do this, the burial history derived

from the stratigraphy of the preserved sedimentary section is used to calculate a thermal history for each sample using the present geothermal gradient and surface temperature (i.e. assuming these have not changed through time). This is termed the "Default Thermal History". For each sample, the AFTA parameters predicted as a result of the Default Thermal History are then compared to the measured data. If the data show a greater degree of annealing than calculated on the basis of this history, the sample must have been hotter at some time in the past. In this case, the AFTA data are analysed to provide estimates of the magnitude of the maximum paleotemperature in that sample, and the time at which cooling commenced from the thermal maximum.

The degree of annealing is assessed in two ways - from fission track age and track length data. The stratigraphic age provides a basic reference point for the interpretation of fission track age, because reduction of the fission track age below the stratigraphic age unequivocally reveals that appreciable annealing has taken place after deposition of the host sediment. Large degrees of fission track age reduction, with the pooled or central fission track age very much less than the stratigraphic age, indicate severe annealing, which requires paleotemperatures of at least ~100°C for any reasonable geological time-scale of heating (>~1 Ma). Note that this applies even when apatites contain tracks inherited from source areas. More moderate degrees of annealing can be detected by inspection of the single grain age data, as the most sensitive (fluorine-rich) grains will begin to give fission track ages significantly less than the stratigraphic age before the central or pooled age has been reduced sufficiently to give a noticeable signal. Note that this aspect of the single grain age data can also be used for apatites which have tracks inherited from source areas. If signs of moderate annealing (from single grain age reduction) or severe annealing (from the reduction in pooled or central age) are seen in samples in which the Default Thermal History predicts little or no effect, the sample must have been subjected to elevated paleotemperatures at some time in the past. Figure C.7 shows how increasing degrees of annealing are observable in radial plots of the single grain fission track age data.

Similarly, the present temperature from which a sample is taken, and the way in which this has been approached (as inferred from the preserved sedimentary section), forms a basic point of reference for track length data. The observed mean track length is compared with the mean length predicted from the Default Thermal History. If the observed degree of track shortening in a sample is greater than that expected from the Default Thermal History (i.e. the mean length is significantly less than the predicted value), either the sample must have been subjected to higher paleotemperatures at some time after deposition, or the sample contains shorter tracks which were inherited from sediment source areas at the time the sediment was deposited. If shorter tracks were

inherited from source areas, the sample should still contain a component of longer tracks corresponding to the tracks formed after deposition. In general, the fission track age should be greater than the stratigraphic age. This can be assessed quantitatively using the computer models for the development of AFTA parameters described in an earlier section. If the presence of shorter tracks cannot be explained by their inheritance from source areas, the sample must have been hotter in the past.

C.5 Quantitative determination of the magnitude of maximum paleotemperature and the timing of cooling using AFTA

Values of maximum paleotemperature and timing of cooling in each sample are determined using a forward modelling approach based on the quantitative description of fission track annealing described in earlier sections. The Default Thermal History described above is used as the basis for this forward modelling, but with the addition of episodes of elevated paleotemperatures as required to explain the data. AFTA parameters are modelled iteratively through successive thermal history scenarios in order to identify thermal histories that can account for observed parameters. The range of values of maximum paleotemperature and timing of cooling which can account for the measured AFTA parameters (fission track age and track length distribution) are defined using a maximum likelihood-based approach. In this way, best estimates ("maximum likelihood values") can be defined together with ±95% confidence limits.

In samples in which all tracks have been totally annealed at some time in the past, only a minimum estimate of maximum paleotemperature is possible. In such cases, AFTA data provide most control on the time at which the sample cooled to temperatures at which tracks could be retained. The time at which cooling began could be earlier than this time, and therefore the timing also constitutes a minimum estimate.

Comparison of the AFTA parameters predicted by the multi-compositional model with measured values in samples which are currently at their maximum temperatures since deposition shows a good degree of consistency, suggesting the uncertainty in application of the model should be less than ±10°C. This constitutes a significant improvement over earlier approaches, since the kinetic models used are constrained in both laboratory and geological conditions. It should be appreciated that relative differences in maximum paleotemperature can be identified with greater precision than absolute paleotemperatures, and it is only the estimation of absolute paleotemperature values to which the ±10°C uncertainty relates.

Cooling history

If the data are of high quality and provided that cooling from maximum paleotemperatures began sufficiently long ago (so that the history after this time is represented by a significant proportion of the total tracks in the sample), determination of the magnitude of a subsequent peak paleotemperature and the timing of cooling from that peak may also be possible (as explained in Section C.2). A similar approach to that outlined above provides best estimates and corresponding ±95% confidence limits for this episode. Such estimates may simply represent part of a protracted cooling history, and evidence for a later discrete cooling episode can only be accepted if this scenario provides a significantly improved fit to the data. Geological evidence and consistency of estimates between a series of samples can also be used to verify evidence for a second episode.

In practise, most typical AFTA datasets are only sufficient to resolve two discrete episodes of heating and cooling. One notable exception to this is when a sample has been totally annealed in an early episode, and has then undergone two (or more) subsequent episodes with progressively lower peak paleotemperatures in each. But in general, complex cooling histories involving a series of episodes of heating and cooling will allow resolution of only two episodes, and the results will depend on which episodes dominate the data. Typically this will be the earliest and latest episodes, but if multiple cooling episodes occur within a narrow time interval the result will represent an approximation to the actual history.

C.6 Qualitative assessment of AFTA parameters

Various aspects of thermal history can often be assessed by qualitative assessment of AFTA parameters. For example, samples which have reached maximum paleotemperatures sufficient to produce total annealing, and which only contain tracks formed after the onset of cooling, can be identified from a number of lines of evidence. In a vertical sequence of samples showing increasing degrees of annealing, the transition from rapidly decreasing fission track age with increasing depth to more or less the same age over a range of depth denotes the transition from partial to total annealing of all tracks formed prior to the thermal maximum. In samples in which all tracks have been totally annealed, the single grain age data should show that none of the individual grain fission track ages are significantly older than the time of cooling, and grains in all compositional groups should give the same fission track age unless the sample has been further disturbed by a later episode. If the sample cooled rapidly to sufficiently low temperatures, little annealing will have taken place since cooling, and all grains will

give ages which are compatible with a single population around the time of cooling, as shown in Figure C.7.

Inspection of the distribution of single grain ages in partially annealed samples can often yield useful information on the time of cooling, as the most easily annealed grains (those richest in fluorine) may have been totally annealed prior to cooling, while more retentive (Cl-rich) compositions were only partially annealed (as in Figure C.7, centre). The form of the track length distribution can also provide information, from the relative proportions of tracks with different lengths. All of these aspects of the data can be used to reach a preliminary thermal history interpretation.

C.7 Allowing for tracks inherited from source areas

The effect of tracks inherited from source areas, and present at the time the apatite is deposited in the host sediment, is often posed as a potential problem for AFTA. However, this can readily be allowed for in analysing both the fission track age and length data.

In assessing fission track age data to determine the degree of annealing, the only criterion used is the comparison of fission track age with the value expected on the basis of the Default Thermal History. From this point of view, inherited tracks do not affect the conclusion: if a grain or a sample gives a fission track age which is significantly less than expected, the grain or sample has clearly undergone a higher degree of annealing than can be accounted for by the Default Thermal History, and therefore must have been hotter in the past, whether the sample contained tracks when it was deposited or not.

The presence of inherited tracks does impose a limit on our ability to detect post-depositional annealing from age data alone, as in samples which contain a fair proportion of inherited tracks, moderate degrees of annealing may reduce the fission track age from the original value, but not to a value which is significantly less than the stratigraphic age. This is particularly noticeable in the case of Tertiary samples containing apatites derived from Paleozoic basement. In such cases, although fission track age data may show no evidence of post-depositional annealing, track length data may well show such evidence quite clearly.

The influence of track lengths inherited from source areas can be allowed for by comparison of the fission track age with the value predicted by the Default Thermal History combined with inspection of the track length distribution. If the mean length is much less than the length predicted by the Default Thermal History, either the sample has been subjected to elevated paleotemperatures, sufficient to produce the observed degree of length reduction, or else the sample contains a large proportion of shorter

tracks inherited from source areas. However, in the latter case, the sample should give a pooled or central fission track age correspondingly older than the stratigraphic age, while the length distribution should contain a component of longer track lengths corresponding to the value predicted by the Default Thermal History. It is important in this regard that the length of a track depends primarily on the maximum temperature to which it has been subjected, whether in the source regions or after deposition in the sedimentary basin. Thus, any tracks retaining a provenance signature will have lengths towards the shorter end of the distribution where track lengths will not have "equilibrated" with the temperatures attained since deposition.

In general, it is only in extreme cases that inherited tracks render track length data insensitive to post-depositional annealing. For example, if practically all the tracks in a particular sample were formed prior to deposition, perhaps in a Pliocene sediment in which apatites were derived from a stable Paleozoic shield with fission track ages of ~300 Ma or more, the track length distribution will, in general, be dominated by inheritance, as only ~2% of tracks would have formed after deposition. Post-depositional heating will not be detectable as long as the maximum paleotemperature is insufficient to cause greater shortening than that which occurred in the source terrain. Even in such extreme cases, once a sample is exposed to temperatures sufficient to produce greater shortening than that inherited from source areas, the inherited tracks and those formed after deposition will all undergo the same degree of shortening, and the effects of post-depositional annealing can be recognised. In such cases, the presence of tracks inherited from source areas is actually very useful, because the number of tracks formed after deposition is so small that little or no information would be available without the inherited tracks.

C.8 Plots of fission track age and mean track length vs depth and temperature

AFTA data from well sequences are usually plotted as shown in Figure C.8. This figure shows AFTA data for two scenarios: one in which deposition has been essentially continuous from the Carboniferous to the present and all samples are presently at their maximum paleotemperature since deposition (Figure C.8a); and, one in which the section was exposed to elevated paleotemperatures prior to cooling in the Early Tertiary (Figure C.8b).

In both figures, fission track age and mean track length are plotted against depth and present temperature. Presentation of AFTA data in this way often provides insight into the thermal history interpretation, following principles outlined earlier in this Appendix.

In Figure C.8a**,** for samples at temperatures below ~70°C, the fission track age is either greater than or close to the stratigraphic age, and little fission track age reduction has affected these samples. Track lengths in these samples are all greater than ~13 µm. In progressively deeper samples, both the fission track age and mean track length are progressively reduced to zero at a present temperature of around 110°C, with the precise value depending on the spread of apatite compositions present in the sample. Track length distributions in the shallowest samples would be a mixture of tracks retaining information on the thermal history of source regions, while in deeper samples, all tracks would be shortened to a length determined by the prevailing temperature. This pattern of AFTA parameters is characteristic of a sequence which is currently at maximum temperatures.

The data in Figure C.8b show a very different pattern. The fission track age data show a rapid decrease in age, with values significantly less than the stratigraphic age at temperatures of ~40 to 50°C, at which such a degree of age reduction could not be produced in any geological timescale. Below this rapid fall, the fission track ages do not change much over ~1 km (30°C). This transition from rapid fall to consistent ages is diagnostic of the transition from partial to total annealing. Samples above the "break-in slope" contain two generations of tracks: those formed prior to the thermal maximum, which have been partially annealed (shortened) to a degree which depends on the maximum paleotemperature; and, those formed after cooling, which will be longer. Samples below the break-in slope contain only one generation of tracks, formed after cooling to lower temperatures at which tracks can be retained. At greater depths, where temperatures increase to ~90°C and above, the effect of present temperatures begins to reduce the fission track ages towards zero, as in the "maximum temperatures now" case.

The track length data also reflect the changes seen in the fission track age data. At shallow depths, the presence of the partially annealed tracks shortened prior to cooling causes the mean track length to decrease progressively as the fission track age decreases. However, at depths below the break in slope in the age profile, the track length increases again as the shorter component is totally annealed and so does not contribute to the measured distribution of track lengths. At greater depths, the mean track lengths decrease progressively to zero once more due to the effects of the present temperature regime.

Examples of such data have been presented, e.g. by Green (1989) and Kamp and Green (1990).

C.9 Determining paleogeothermal gradients and amount of section removed on unconformities

Estimates of maximum paleotemperatures in samples over a range of depths in a vertical sequence provides the capability of determining the paleogeothermal gradient immediately prior to the onset of cooling from those maximum paleotemperatures. The degree to which the paleogeothermal gradient can be constrained depends on a number of factors, particularly the depth range over which samples are analysed. If samples are only analysed over ~1 km, then the paleotemperature difference over that range may be only ~20 to 30°C. Since maximum paleotemperatures can often only be determined within a ~10°C range, this introduces considerable uncertainty into the final estimate of paleogeothermal gradient (see Figure C.9).

Another important factor is the difference between maximum paleotemperatures and present temperatures ("net cooling"). If this is only ~10°C, which is similar to the uncertainty in absolute paleotemperature determination, only broad limits can be established on the paleogeothermal gradient. In general, the control on the paleogeothermal gradient improves as the amount of net cooling increases. However, if the net cooling becomes so great that many samples were totally annealed prior to the onset of cooling - so that only minimum estimates of maximum paleotemperatures are possible - constraints on the paleogeothermal gradient from AFTA come only from that part of the section in which samples were not totally annealed. In this case, integration of AFTA data with VR measurements can be particularly useful in constraining the paleo-gradient.

Having constrained the paleogeothermal gradient at the time cooling from maximum paleotemperatures began, if we assume a value for surface temperature at that time, the amount of section subsequently removed by uplift and erosion can be calculated as shown in Figure C.10. The *net* amount of section removed is obtained by dividing the difference between the paleo-surface temperature (T_S) and the intercept of the paleotemperature profile at the present ground surface (T_i) by the estimated paleogeothermal gradient. The *total* amount of section removed is obtained by adding the thickness of section subsequently redeposited above the unconformity to the *net* amount estimated as in Figure C.10. If the analysis is performed using depths from the appropriate unconformity, then the analysis will directly yield the *total* amount of section removed.

Geotrack have developed a method of deriving estimates of both the paleogeothermal gradient and the net amount of section removed using estimated paleotemperatures

derived from AFTA and VR. Perhaps more importantly, this method also provides rigorous values for upper and lower 95% confidence limits on each parameter. The method is based on maximum likelihood estimation of the paleogeothermal gradient and the surface intercept, from a table of paleotemperature and depth values. The method is able to accept ranges for paleotemperature estimates (e.g. where the maximum paleotemperature can only be constrained to between, for example, 60 and 90°C), as well as upper and lower limits (e.g. <60°C for samples which show no detectable annealing; >110°C in samples which were totally annealed). Estimates of paleotemperature from AFTA and VR may be combined or analysed separately. Some results from this method have been reported by Bray et al. (1992). Full details of the methods employed are presented in a confidential, in-house, Geotrack research report, copies of which are available on request from the Melbourne office.

Results are presented in two forms. Likelihood profiles, plotting the log-likelihood as a function of either gradient or section removed, portray the probability of a given value of gradient or section removed. The best estimate is given by the value of gradient or section removed for which the log-likelihood is maximised. Ideally, the likelihood profiles should show a quadratic form, and values of gradient or section removed at which the log-likelihood has fallen by two from the maximum value define the upper and lower 95% confidence limits on the estimates. An alternative method of portraying this information is a crossplot of gradient against section removed, in which values which fall within 95% confidence limits (in two dimensions) are contoured. Note that the confidence limits defined by this method are rather tighter than those from the likelihood profiles, as the latter only reflect variation in one parameter, whereas the contoured crossplot takes variation of both parameters into account.

It must be emphasised that this method relies on the assumption that the paleotemperature profile was linear both throughout the section analysed and through the overlying section which has been removed. While the second part of this assumption can never be confirmed independently, visual inspection of the paleotemperature estimates as a function of depth should be sufficient to verify or deny the linearity of the paleotemperature profile through the preserved section.

Results of this procedure are shown in this report if the data allow sufficiently well-defined paleotemperature estimates to justify use of the method. Where the AFTA data suggest that the section is currently at maximum temperature since deposition, or that the paleotemperature profile was non-linear, or where data are of insufficient quality to allow rigorous paleotemperature estimation, the method is not used.

References

Carlson, W.D. (1990) Mechanisms and kinetics of apatite fission-track annealing. *American Mineralogist*, 75, 1120 - 1139.

Corrigan, J. (1992) Annealing models under the microscope, *On Track*, 2, 9-11.

Crowley, K.D., Cameron, M. and Schaefer, R.L. (1991) Experimental studies of annealing of etched fission tracks in apatite. *Geochimica et Cosmochimica Acta*, 55, 1449-1465.

Duddy, I.R., Green, P.F. and Laslett G.M. (1988) Thermal annealing of fission tracks in apatite 3. Variable temperature behaviour. *Chem. Geol. (Isot. Geosci. Sect.)* , 73, 25-38.

Gleadow, A.J.W. and Duddy, I.R. (1981) A natural long-term track annealing experiment for apatite. *Nuclear Tracks*, 5, 169-174.

Gleadow, A.J.W., Duddy, I.R. and Lovering, J.F. (1983) Fission track analysis; a new tool for the evaluation of thermal histories and hydrocarbon potential. *APEA J,* 23, 93-102.

Gleadow, A.J.W., Duddy, I.R., Green, P.F. and Lovering, J.F. (1986) Confined fission track lengths in apatite - a diagnostic tool for thermal history analysis. *Contr. Min. Petr.*, 94, 405-415.

Green, P.F. (1988) The relationship between track shortening and fission track age reduction in apatite: Combined influences of inherent instability, annealing anisotropy, length bias and system calibration. *Earth Planet. Sci. Lett.*, 89, 335-352.

Green, P.F., Duddy, I.R., Gleadow, A.J.W., Tingate, P.R. and Laslett, G.M. (1986) Thermal annealing of fission tracks in apatite 1. A qualitative description. *Chem. Geol. (Isot. Geosci. Sect.)* , 59, 237-253.

Green, P.F., Duddy, I.R., Gleadow, A.J.W. and Lovering, J.F. (1989a) Apatite Fission Track Analysis as a paleotemperature indicator for hydrocarbon exploration. *In:* Naeser, N.D. and McCulloh, T. (eds.) *Thermal history of sedimentary basins - methods and case histories*, Springer-Verlag, New York, 181-195.

Green, P.F., Duddy, I.R., Laslett, G.M., Hegarty, K.A., Gleadow, A.J.W. and Lovering, J.F. (1989b) Thermal annealing of fission tracks in apatite 4. Quantitative modelling techniques and extension to geological timescales. *Chem. Geol. (Isot. Geosci. Sect.)*, 79, 155-182

Green, P.F., Laslett, G.M. and Duddy, I.R. (1993) Mechanisms and kinetics of apatite fission track annealing: Discussion. *American Mineralogist*, 78, 441-445.

Laslett, G.M., Kendall, W.S., Gleadow, A.J.W. and Duddy, I.R. (1982) Bias in measurement of fission track length distributions. *Nuclear Tracks*, 6, 79-85.

Laslett, G.M., Green, P.F., Duddy, I.R. and Gleadow, A.J.W. (1987) Thermal annealing of fission tracks in apatite 2. A quantitative analysis. *Chem. Geol. (Isot. Geosci. Sect.)*, 65, 1-13.

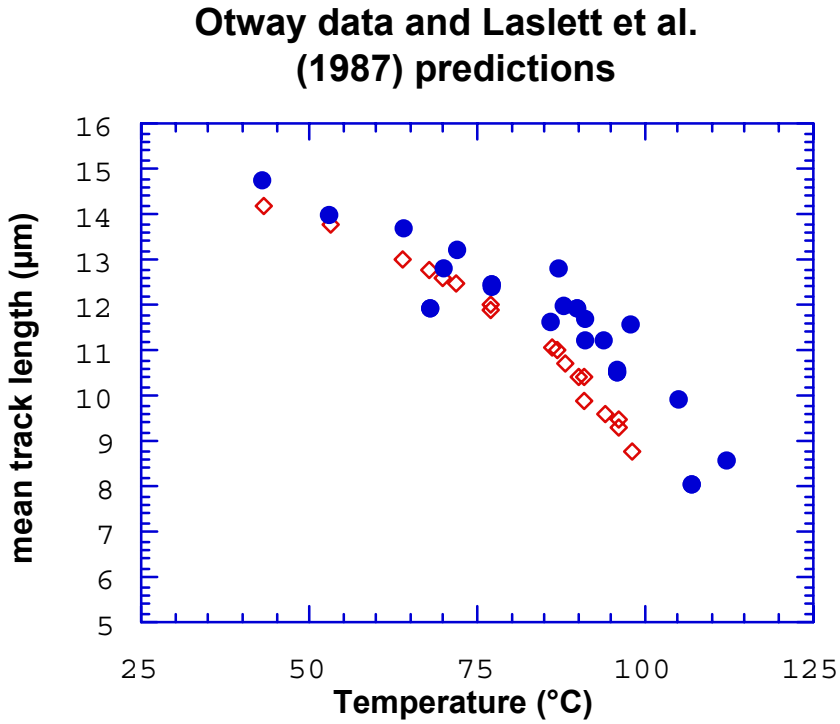

Figure C.1a Comparison of mean track length (solid circles) measured in samples from four Otway Basin reference wells (from Green et al, 1989a) and predicted mean track lengths (open diamonds) from the kinetic model of fission track annealing from Laslett et al. (1987). The predictions underestimate the measured values, but they refer to an apatite composition that is more easily annealed than the majority of apatites in these samples, so this is expected.

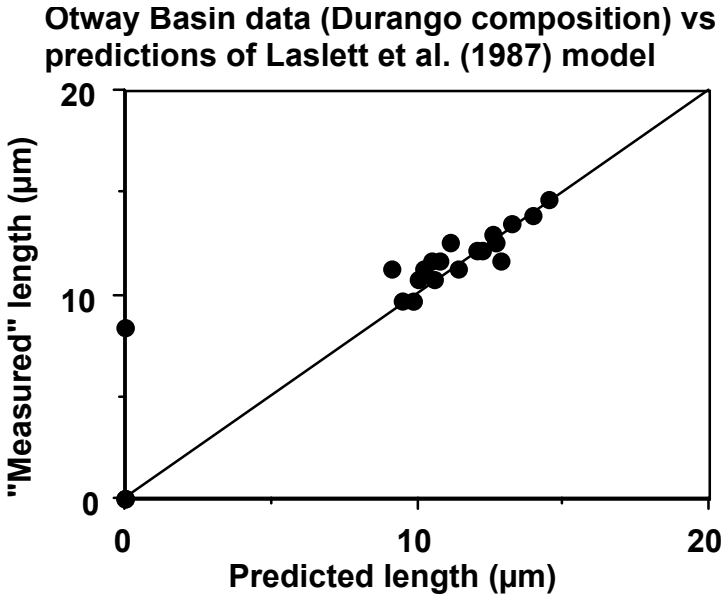

Figure C.1b Comparison of the mean track length in apatites of the same Cl content as Durango apatite from the Otway Group samples illustrated in figure C.1a, with values predicted for apatite of the same composition by the model of Laslett et al. (1987). The agreement is clearly very good except possibly at lengths below ~10 µm.

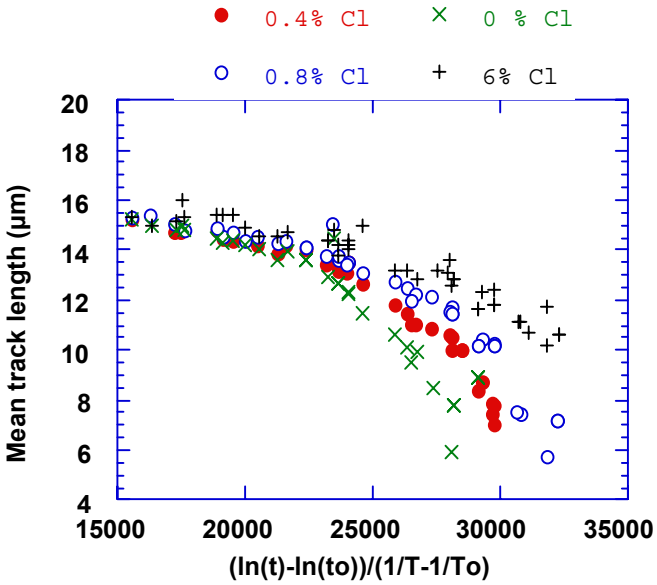

Figure C.2 Mean track length in apatites with four different chlorine contents, as a combined function of temperature and time, to reduce the data to a single scale. Fluorapatites are more easily annealed than chlorapatites, and the annealing kinetics show a progressive change with increasing Cl content.

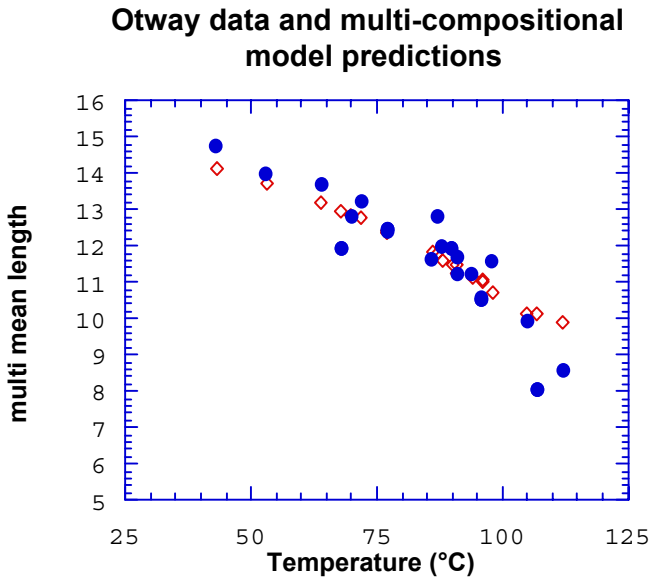

Figure C.3 Comparison of measured mean track length (solid circles) in samples from four Otway Basin reference wells (from Green et al, 1989a) and predicted mean track lengths (open diamonds) from the new multi-compositional kinetic model of fission track annealing described in Section C.3. This model takes into account the spread of Cl contents in apatites from the Otway Group samples and the influence of Cl content on annealing rate. The agreement is clearly very good over the range of the data.

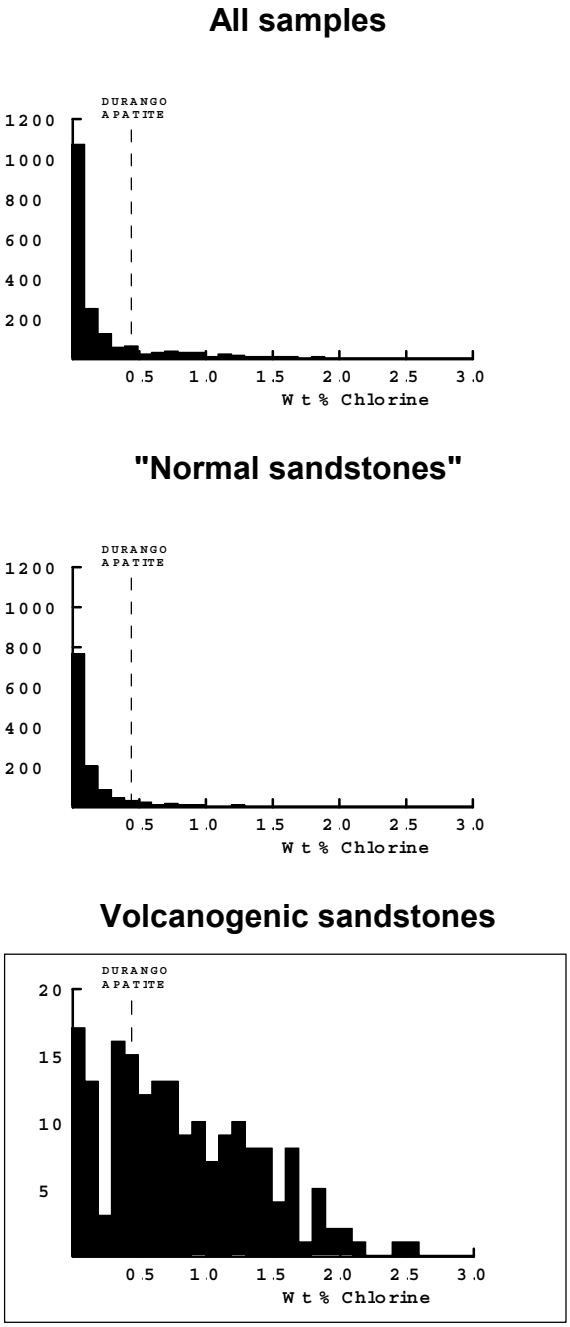

Figure C.4 **a:** Histogram of Cl contents (wt%) in over 1750 apatite grains from over 100 samples of various sedimentary and igneous rocks. Most samples give Cl contents below ~0.5 wt %, while those apatites giving higher Cl contents are characteristic of volcanogenic sandstones and basic igneous sources.

b: Histogram of Cl contents (wt%) in 1168 apatite grains from 61 samples which can loosely be characterised as "normal sandstone". The distribution is similar to that in the upper figure, except for a lower number of grains with Cl contents greater than ~1%.

c: Histogram of Cl contents (wt%) in 188 apatite grains from 15 samples of volcanogenic sandstone. The distribution is much flatter than the other two, with much higher proportion of Cl-rich grains.

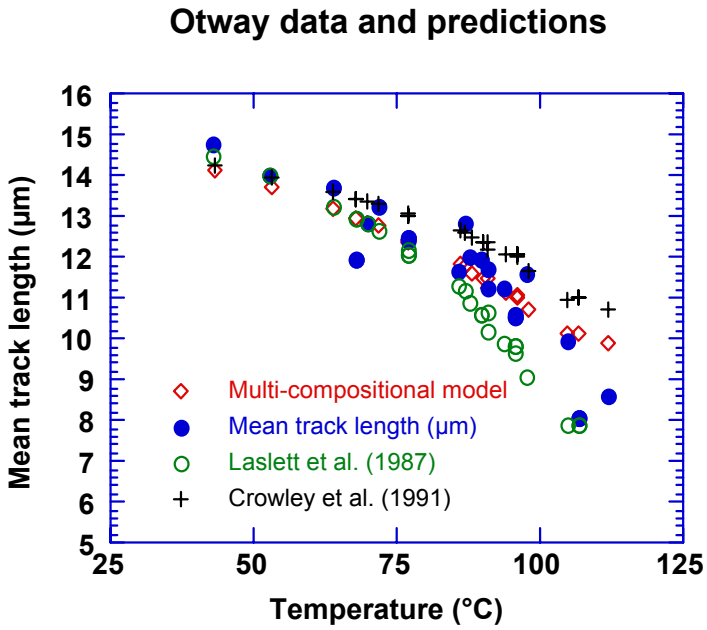

Figure C.5 Comparison of mean track length in samples from four Otway Basin reference wells (from Green et al, 1989a) and predicted mean track lengths from three kinetic models for fission track annealing. The Crowley et al. (1991) model relates to almost pure Fluorapatite (B-5), yet overpredicts mean lengths in the Otway Group samples which are dominated by Cl-rich apatites. The predictions of that model are therefore not reliable.

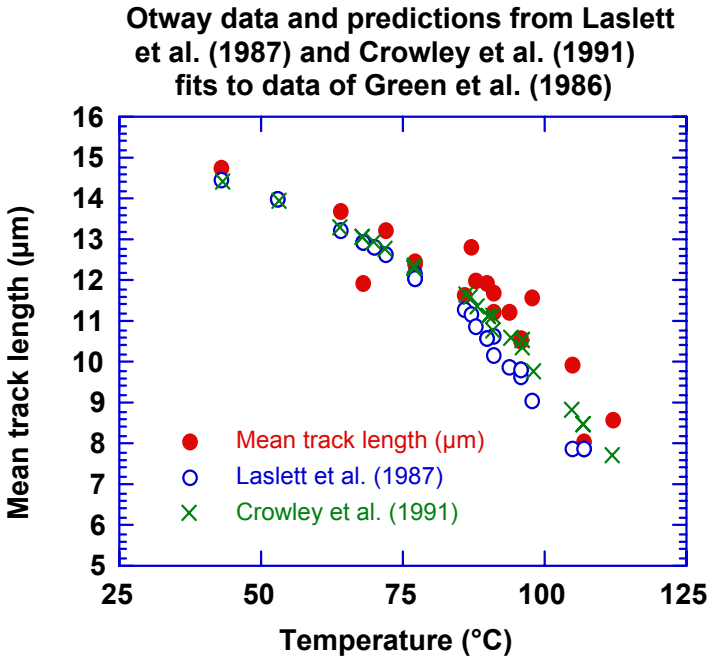

Figure C.6 Comparison of mean track length in samples from four Otway Basin reference wells with values predicted from Laslett et al. (1987) and the model fitted to the annealing data of Green et al. (1986) by Crowley et al. (1991). The predictions of the two models are not very different.

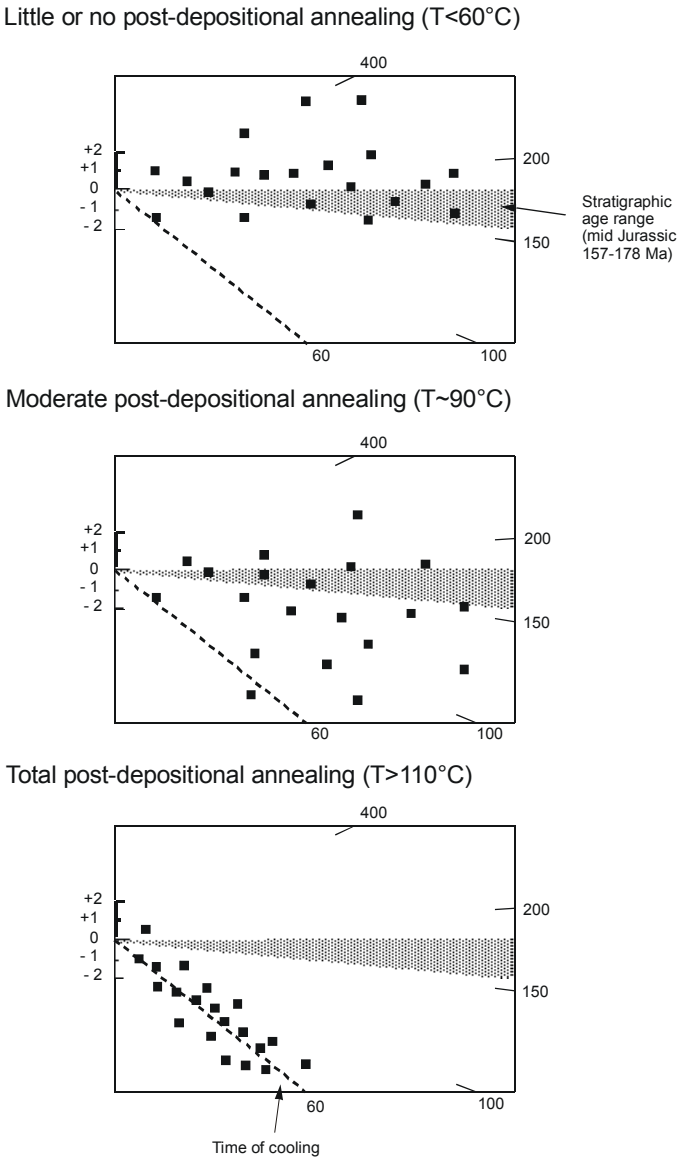

Figure C.7 Radial plots of single grain age data in three samples of mid-Jurassic sandstone that have been subjected to varying degrees of post-depositional annealing prior to cooling at ~60 Ma. The mid-point of the stratigraphic age range has been taken as the reference value (corresponding to the horizontal).

The upper diagram represents a sample which has remained at paleotemperatures less than ~60°C, and has therefore undergone little or no post-depositional annealing. All single grain ages are either compatible with the stratigraphic age (within y = ±2 in the radial plot) or older than the stratigraphic age ($y_i > 2$).

The centre diagram represents a sample which has undergone a moderate degree of post-depositional annealing, having reached a maximum paleotemperature of around ~90°C prior to cooling. While some of the individual grain ages are compatible with the stratigraphic age ($-2 < y_i < +2$) and some may be significantly greater than the stratigraphic age ($y_i > 2$), a number of grains give ages which are significantly less than the stratigraphic age ($y < 2$).

The lower diagram represents a sample in which all apatite grains were totally annealed, at paleotemperatures greater than ~110°C, prior to rapid cooling at ~60 Ma. All grains give fission track ages compatible with a fission track age of ~60 Ma (i.e., all data plot within ±2 of the radial line corresponding to an age of ~60 Ma), and most are significantly younger than the stratigraphic age.

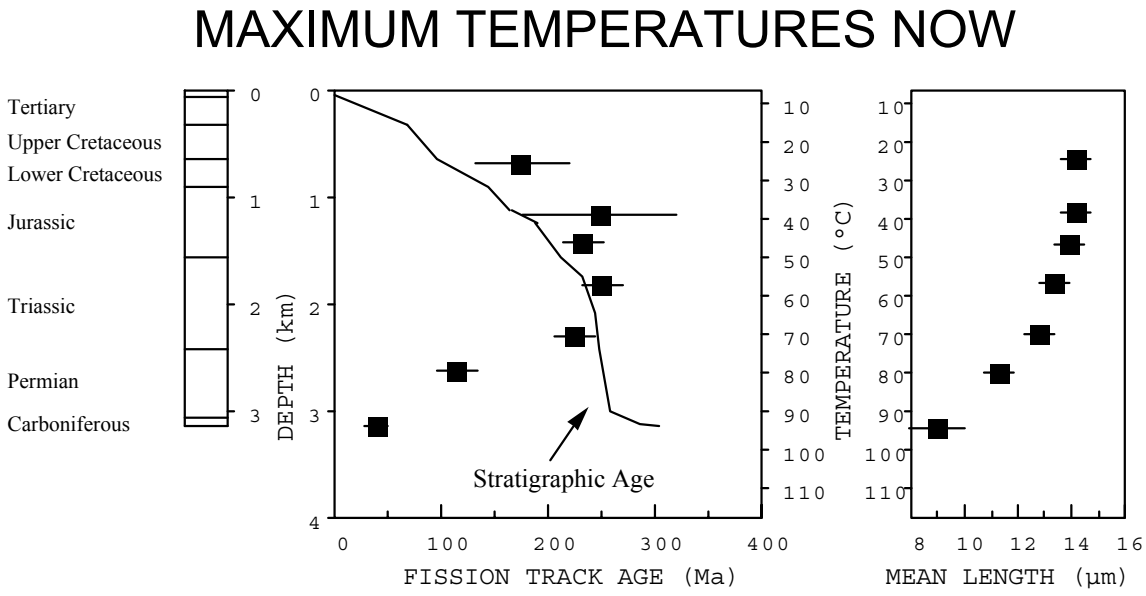

Figure C.8a Typical pattern of AFTA parameters in a well in which samples throughout the entire section are currently at their maximum temperatures since deposition. Both the fission track age and mean track length undergo progressive reduction to zero at temperatures of ~100 - 110°C, the actual value depending on the range of apatite compositions present.

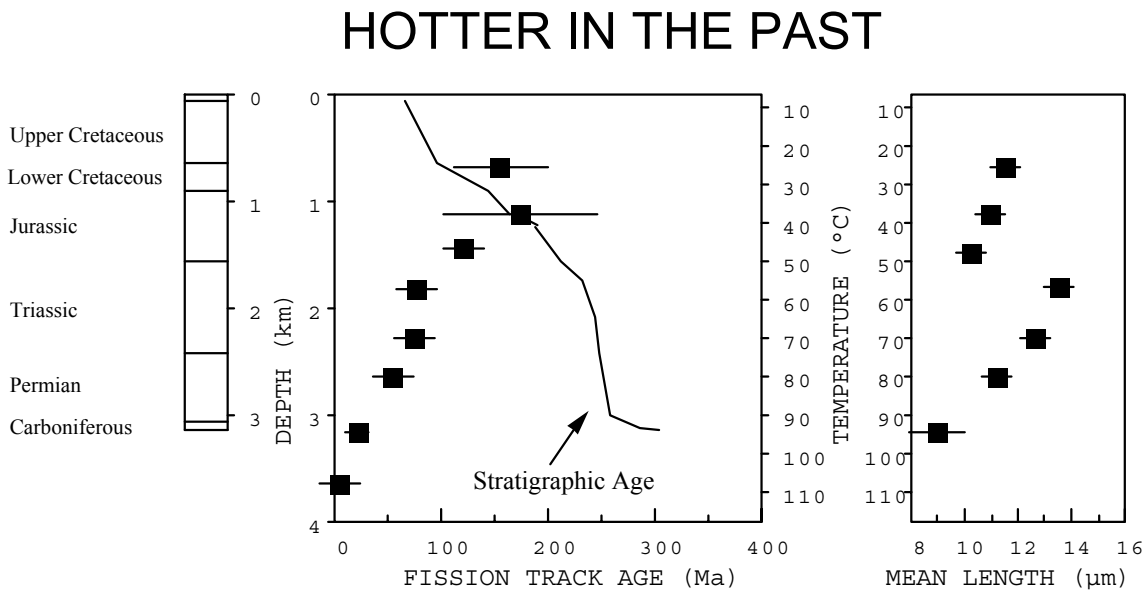

Figure C.8b Typical pattern of AFTA parameters in a well in which samples throughout the section were exposed to elevated paleotemperatures after deposition (prior to cooling in the Early Tertiary, in this case). Both the fission track age and mean track length show more reduction at temperatures of ~40 to 50°C than would be expected at such temperatures. At greater depths (higher temperatures), the constancy of fission track age and the increase in track length are both diagnostic of exposure to elevated paleotemperatures. See Appendix C for further discussion

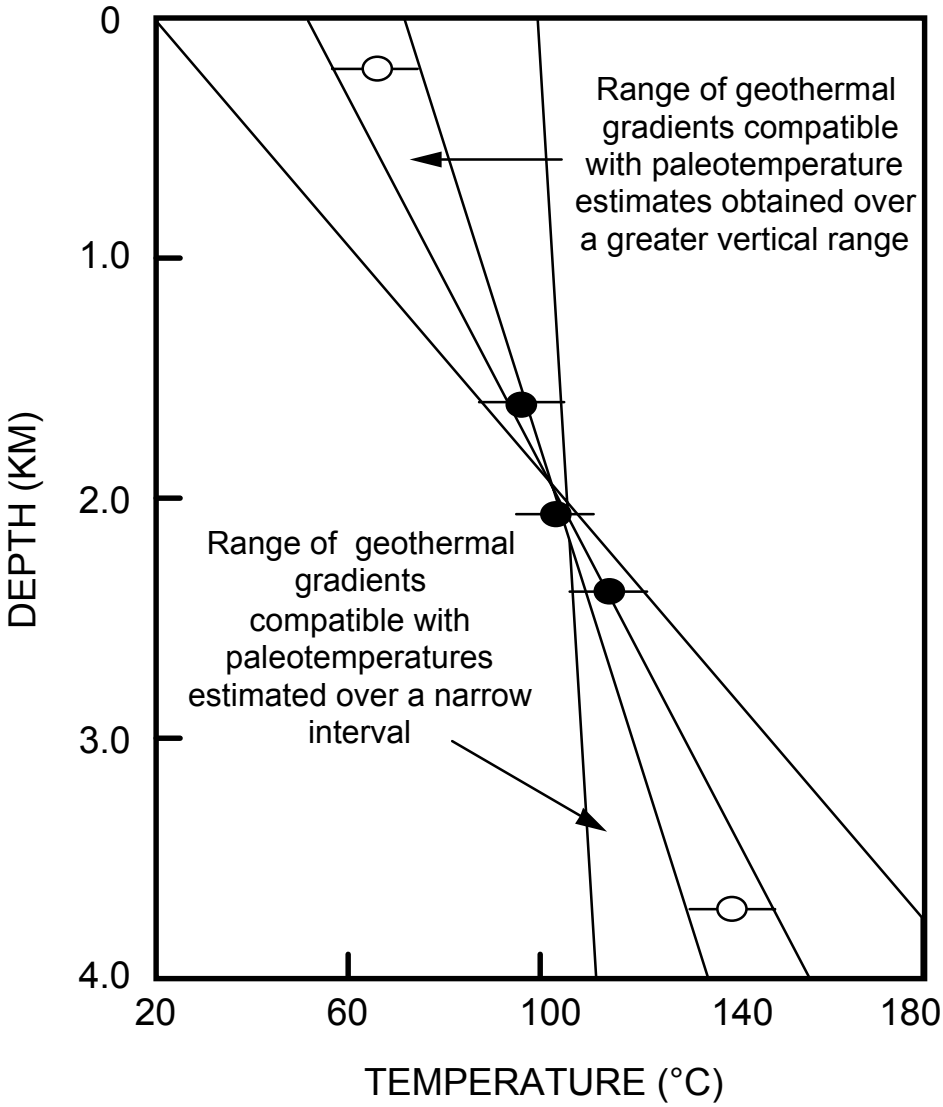

Figure C.9 It is important to obtain paleotemperature constraints over as great a range of depths as possible in order to provide a reliable estimate of paleogeothermal gradient. If paleotemperatures are only available over a narrow depth range, then the paleogeothermal gradient can only be very loosely constrained.

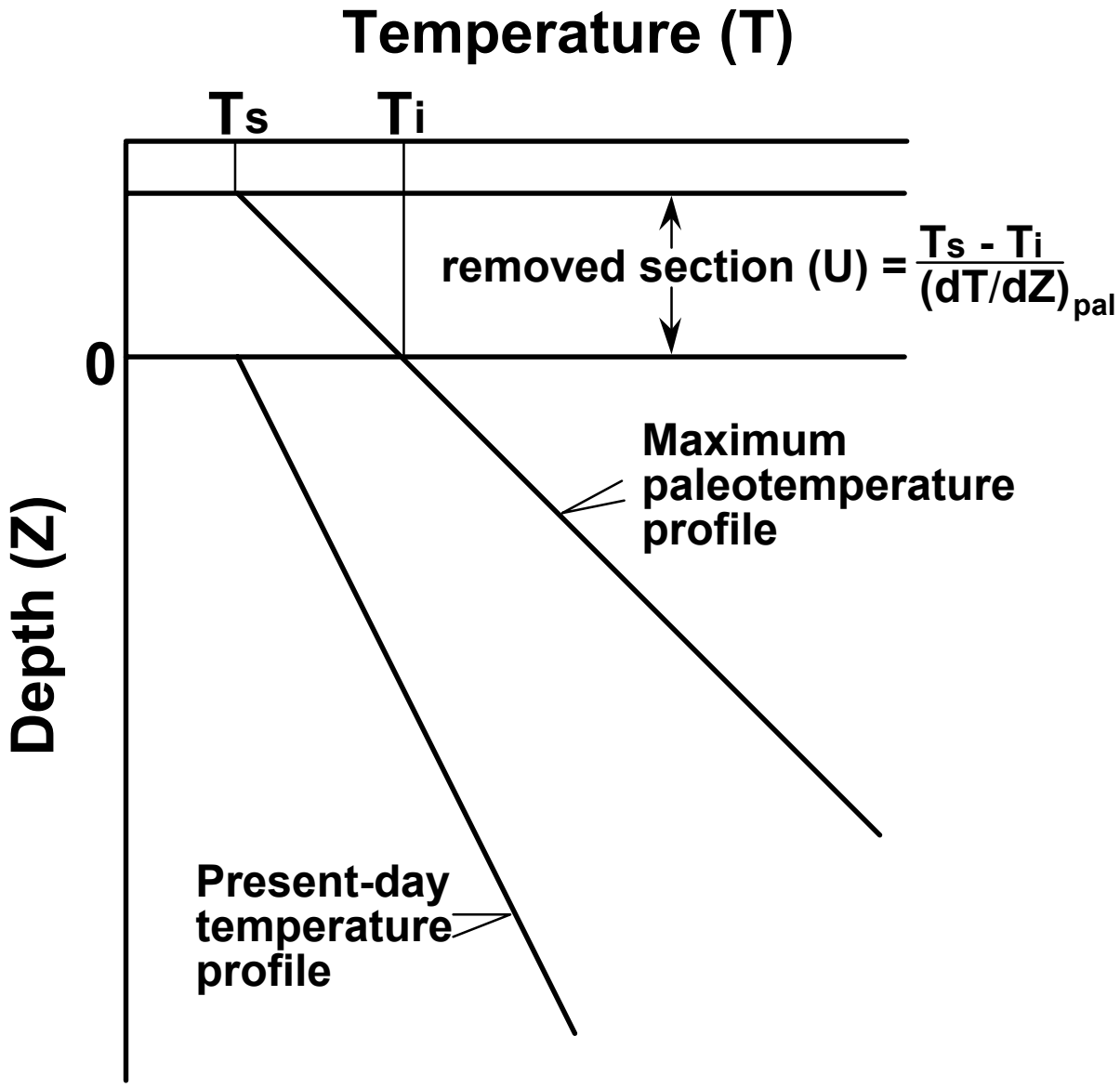

Figure C.10 If the paleogeothermal gradient can be constrained by AFTA and VR, as explained in the text, then for an assumed value of surface temperature, T_S, the amount of section removed can be estimated, as shown.

APPENDIX D

Vitrinite Reflectance Measurements

D.1 New vitrinite reflectance determinations

No new vitrinite reflectance data were collected as part of this study, but a suite of 7 VR determinations were supplied by the client for assessment. These VR data were sourced from Geotech Pty Ltd and were ultimately collected by Prof. Alan Cook of Keiraville Konsultants Pty Ltd. The methodology employed by Keiraville Konsultants is described in sections D.1 and D.2 below.

Samples

Vitrinite reflectance results and sample details are summarised in Table D.2, while supporting data, including maceral descriptions and raw data sheets, are presented in the following pages.

Equipment

Leitz MPV1.1 photometer equipped with separate fluorescence illuminator, Swift point counter. Reflectance standards: spinel 0.42%, YAG 0.91%, GGG 1.72%, SiC standard for cokes and masked uranyl glass for measurement of intensity (I) in fluorescence mode. With the Keiraville Konsultants equipment, it is possible to alternate from reflectance to fluorescence mode to check for associated fluorescing liptinite, or importantly with some samples, to check for bitumen impregnation, or the presence, intensity, and source of oil-cut.

Sample preparation

Samples are normally mounted in cold setting polyester resin and polished using Cr_2O_3 and Mg0 polishing powders. Epoxy resins or araldite can be used if required. "Whole rock" samples are normally used but demineralisation can be undertaken. Large samples of coals and cokes can be mounted and examined.

Vitrinite Reflectance measurement

The procedure used generally follows Australian Standard (AS) 2486, but has been slightly modified for use with dispersed organic matter (DOM). For each sample, a minimum of 25 fields is measured (the number may be less if vitrinite is rare or if a limited number of particles of vitrinite is supplied, as may be the case with hand-picked

samples). If wide dispersal of vitrinite reflectance is found, the number of readings (N) is increased until a stable mean is obtained.

Vitrinite identification is made primarily on textural grounds, and this allows an independent assessment to be made of cavings and re-worked vitrinite populations. Histograms are only used for population definition when a cavings population significantly overlaps the range of the indigenous population. Where such data provides additional information, the mean maximum reflectance of inertinite and/or the mean maximum reflectance of liptinite (exinite) is reported. For each field, the maximum reflectance position is located and the reading recorded. The stage is then rotated by 180° which should give the same reading. In practice, the readings are seldom identical because of stage run-out and slight surface irregularities. If the readings are within ±5% relative, they are accepted. If not, the cause of the difference is sought and the results rejected. The usual source of differences is surface relief. The measurement of both maxima results in a total of 50 measurements being taken for the 25 fields reported. Thus, the 50 readings consist of 25 pairs of closely spaced readings which provide a check on the levelling of the surface and hence additional precision.

As the vitrinite reflectance measurements are being made, the various features of the samples are noted on a check sheet to allow a sample description to be compiled. When the reflectance measurements are complete, a thorough check is made of liptinite fluorescence characteristics. At the same time, organic matter abundance is estimated using a global estimate, a grain count method or point count method as required.

Data presentation

Individual sample results are reported in the following format:

KK#[*1] Ref#[*2]	Depth (ft)	R_V max[*3]	Range[*4]	N[*5]
v1324	3106	0.79	0.64 - 0.91	25
873-1.1	$R_I$max[*6]	1.68	1.02 – 1.98	12

*1 Keiraville Konsultant reference number
*2 Geotrack sample number
*3 Mean of all the maximum reflectance readings obtained.
*4 Lowest $R_o$max and highest $R_o$max of the population considered to represent the first generation vitrinite population.
*5 Number of fields measured (Number of measurements = 2N because 2 maximum values are recorded for each field).
*6 Reflectance of the inertinite maceral (if present) – can be used to estimate an equivalent VR level as shown in Table D.1B.

Methods - Organic matter abundance and type.

After completion of vitrinite reflectance readings, the microscope is switched to fluorescence-mode and an estimate made of the abundance of each liptinite maceral. Fluorescence colours are also noted (BG 3 long UV excitation, TK400 dichroic mirror and a K490 barrier filter). The abundances are estimated using comparison charts. The categories used for liptinite (and other components) are:

Descriptor	%	Source potential
Absent	0	None
Rare	<0.1	Very poor
Sparse	0.1<x<0.5	Poor to fair
Common	0.5<x<2.0	Fair to good
Abundant	2.0<x<10.0	Good to very good
Major	10.0<x<40.0	Very good (excellent if algal)
Dominant	>40.0	Excellent

Dispersed Organic Matter (DOM) composition

At the same time as liptinite abundances are estimated, total DOM, vitrinite and inertinite abundances are estimated and reported in the categories listed above. Liptinite (exinite) fluorescence intensity and colour, lithology and a brief description of organic matter type and abundance are also recorded in a further column. Coal is described separately from dispersed organic matter (DOM). These data can be used to estimate the specific yield of the DOM and form a valuable adjunct to TOC data.

Lithological composition

The lithological abundances are ranked. For cuttings, these data can be useful in conjunction with geophysical logs in assessing the abundance and nature of cavings. For cores, it provides a record of the lithology examined and of the lithological associations of the organic matter.

Coal abundance and composition

Where coals are present, their abundance is recorded and their composition is reported as microlithotypes thus:

Coal major, **V**itrinite>**I**nertinite>**E**xinite, Clarodurite>vitrite>clarite>inertite.

These data give an approximate maceral composition and information about the organic facies of the coal. Where coal is a major or dominant component, and more precise maceral composition data are required, point count analyses should be requested.

However, the precision of the original sampling is commonly a limiting factor in obtaining better quality data.

Abundance factor analysis

Especially where cuttings samples are used, abundance factor analyses are used to obtain an assessment of the maceral assemblages in the various lithologies. This can be done by a combination analysis using a point counter, but a large number of categories is required, and the precision is low if DOM is less than about 10%. For an abundance factor analysis (for core, 50 microscope fields of view) we assess the abundance of DOM, coal and shaly coal in 50 grains. The data can be used to plot DOM and coal abundance profiles.

Analyst/Advisor: Professor A.C. Cook

Prior to transmittal of final results, all samples are examined and checked by A.C. Cook who has more than 30 years' experience of work on coals, cokes, source rocks and source rock maturation.

D.2 Integration of vitrinite reflectance data with AFTA

Vitrinite reflectance is a time-temperature indicator governed by a kinetic response in a similar manner to the annealing of fission tracks in apatite as described in Appendix C. In this study, vitrinite reflectance data are interpreted on the basis of the distributed activation energy model describing the evolution of VR with temperature and time described by Burnham and Sweeney (1989), as implemented in the BasinMod™ software package of Platte River Associates. In a considerable number of wells from around the world, in which AFTA has been used to constrain the thermal history, we have found that the Burnham and Sweeney (1989) model gives good agreement between predicted and observed VR data, in a variety of settings.

As in the case of fission track annealing, it is clear from the chemical kinetic description embodied in equation 2 of Burham and Sweeney (1989) that temperature is more important than time in controlling the increase of vitrinite reflectance. If the Burham and Sweeney (1989) distributed activation energy model is expressed in the form of an Arrhenius plot (a plot of the logarithm of time versus inverse absolute temperature), then the slopes of lines defining contours of equal vitrinite reflectance in such a plot are very similar to those describing the kinetic description of annealing of fission tracks in Durango apatite developed by Laslett et al. (1987), which is used to interpret the AFTA data in this report. This feature of the two quite independent approaches to thermal history analysis means that for a particular sample, a given degree of fission track

annealing in apatite of Durango composition will be associated with the same value of vitrinite reflectance regardless of the heating rate experienced by a sample. Thus paleotemperature estimates based on either AFTA or VR data sets should be equivalent, regardless of the duration of heating. As a guide, Table D.1A gives paleotemperature estimates for various values of VR for two different heating times.

One practical consequence of this relationship between AFTA and VR is, for example, that a VR value of 0.7% is associated with total annealing of all fission tracks in apatite of Durango composition, and that total annealing of all fission tracks in apatites of more Chlorine-rich composition is accomplished between VR values of 0.7 and ~0.9%.

Furthermore, because vitrinite reflectance continues to increase progressively with increasing temperature, VR data allow direct estimation of maximum paleotemperatures in the range where fission tracks in apatite are totally annealed (generally above ~110°C) and where therefore AFTA only provides minimum estimates. Maximum paleotemperature estimates based on vitrinite reflectance data from a well in which most AFTA samples were totally annealed will allow constraints on the paleogeothermal gradient that would not be possible from AFTA alone. In such cases the AFTA data should allow tight constraints to be placed on the time of cooling and also the cooling history, since AFTA parameters will be dominated by the effects of tracks formed after cooling from maximum paleotemperatures. Even in situations where AFTA samples were not totally annealed, integration of AFTA and VR can allow paleotemperature control over a greater range of depth, e.g. by combining AFTA from sand-dominated units with VR from other parts of the section, thereby providing tighter constraint on the paleogeothermal gradient.

Equivalent vitrinite reflectance estimation from inertinite reflectance

Inertinite is another common organic maceral with a reflectance higher than that of vitrinite. The relationship between vitrinite and inertinite reflectance can be rather variable from province to province and with stratigraphic age and there is no universal kinetic relationship available. However, comparison of vitrinite and inertinite reflectance from the same samples has allowed Geotrack to develop a reasonable calibration to provide an equivalent vitrinite reflectance level from inertinite reflectance. The correlation table is provided in Table D.1B.

Equivalent vitrinite reflectance estimation from Rock-Eval Tmax

A correlation table is provided in Table D.1C. This calibration is a generally accepted relationship that can provide reasonable maturity estimates when used with care, as it is known that T_{max} varies with kerogen type at the same level of maturity. In general, we recommend the use of T_{max} as a maturity indicator only when vitrinite reflectance data cannot be obtained. For this report, Rock-Eval T_{max} data are provided in Appendix A.

References

Burnham, A.K. and Sweeney, J.J. (1989). A chemical kinetic model of vitrinite reflectance maturation. *Geochim. et Cosmochim. Acta*, 53, 2649-2657.

Laslett, G.M., Green, P.F., Duddy, I.R. and Gleadow, A.J.W. (1987). Thermal annealing of fission tracks in apatite 2. A quantitative analysis. *Chem. Geol. (Isot. Geosci.Sect.)*, 65, 1-13.

Table D.1A: Paleotemperature - vitrinite reflectance nomogram based on Equation 2 of Burnham and Sweeney (1989)

Paleotemperature (°C / °*F*)	Vitrinite Reflectance (%) 1 Ma Duration of heating	10 Ma Duration of heating
40 / *104*	0.29	0.32
50 / *122*	0.31	0.35
60 / *140*	0.35	0.40
70 / *158*	0.39	0.45
80 / *176*	0.43	0.52
90 / *194*	0.49	0.58
100 / *212*	0.55	0.64
110 / *230*	0.61	0.70
120 / *248*	0.66	0.78
130 / *266*	0.72	0.89
140 / *284*	0.81	1.04
150 / *302*	0.92	1.20
160 / *320*	1.07	1.35
170 / *338*	1.23	1.55
180 / *356*	1.42	1.80
190 / *374*	1.63	2.05
200 / *392*	1.86	2.33
210 / *410*	2.13	2.65
220 / *428*	2.40	2.94
230 / *446*	2.70	3.23

Table D.1B: Equivalent vitrinite reflectance estimated from inertinite reflectance (Geotrack unpublished correlation).

Measured Inertinite Reflectance (%)	Calculated Vitrinite Reflectance (%)
0.88	0.27
0.95	0.3
1.14	0.4
1.31	0.5
1.45	0.6
1.57	0.7
1.68	0.8
1.78	0.9
1.87	1.0
1.97	1.1
2.07	1.2
2.18	1.3
2.31	1.4
2.46	1.5
2.63	1.6
2.84	1.7
3.08	1.8
3.37	1.9
3.70	2.0
4.20	3.0
6.00	5.0

Table D.1C: Equivalent vitrinite reflectance estimated from Rock-Eval Tmax

Ro(max) (%)	Tmax (°C)
0.30	415
0.36	418
0.41	421
0.45	423
0.50	426
0.55	429
0.61	432
0.66	435
0.70	437
0.75	440
0.84	445
0.93	450
1.02	455
1.10	460
1.19	465
1.28	470
1.46	480
1.55	485
1.64	490

Table D.2: Vitrinite reflectance sample details and results supplied by client - Megascolides-1, Gippsland Basin (Geotrack Report #938)

Source number	Depth (m)	Sample type	Stratigraphic Subdivision	Stratigraphic age (Ma)	Present temperature *1 (°C)	VR (Range) %	N
Megascolides-1							
	240	cuttings	Strezlecki C. striatus	108-107	25	0.55 (0.47-0.64)	25
	240	cuttings			25	1.41*² (1.02-2.16)	10
	685	cuttings	Strezlecki C. huglesi	115-108	44	0.66 (0.55-0.75)	25
	685	cuttings			44	1.56*² (1.26-2.16)	10
	1019	core	Strezlecki C. huglesi	115-108	59	0.71 (0.65-0.80)	25
	1019	core			59	1.54*² (1.06-2.04)	10
	1104	core	Strezlecki C. huglesi	115-108	63	0.83 (0.70-0.90)	25
	1535	cuttings	Strezlecki U.F. wonthagensis	123-115	81	0.79 (0.67-0.88)	25
	1535	cuttings			81	1.66*² (1.12-2.86)	6
	1820	cuttings	Strezlecki U.F. wonthagensis	123-115	94	0.86 (0.71-1.01)	6
	1820	cuttings			94	1.78*² (1.26-2.52)	25
	1920	core	Strezlecki U.F. wonthagensis	123-115	98	1.15 (1.08-1.21)	4
	1920	core			98	1.91*² (1.46-2.60)	25

Note: Some samples may contain both vitrinite and inertinite. Only vitrinite data is shown.

*1 See Appendix A for discussion of present temperature data.

*2 Inertinite

VITRINITE REFLECTANCE MEASUREMENT

MEGASCOLIDES-1

Sample Details		Mean	Range	Std Dev	N° of Readings	Sample Description Including Liptinite Fluorescence, Maceral Abundances, Mineral Fluorescence
240.0m	$R_v$max	0.55	0.47-0.64	0.047	25	Common sporinite and rare liptodetrinite orange to dull
Ctgs	$R_I$max	1.41	1.02-2.16	0.363	10	orange, sparse suberinite weak brown, rare cutinite orange. (Siltstone>claystone>shaly coal>coal> sandstone. Shaly coal abundant, V>L>I, vitrite>clarite>duroclarite. Coal sparse, V>L>I, vitrite>clarite>duroclarite. Dom sparse, I>L>V. Inertinite sparse, liptinite and vitrinite rare. Mineral fluorescence moderate to weak orange. Iron oxides rare. Pyrite rare.)
685.0m	$R_v$max	0.66	0.55-0.75	0.044	25	Common sporinite and rare liptodetrinite orange to dull
Ctgs	$R_I$max	1.56	1.26-2.16	0.228	10	orange, sparse suberinite weak brown, rare cutinite orange, rare resinite orange, rare lamalginite orange. (Siltstone>claystone>coal>shaly coal. Coal abundant, V>I>L, duroclarite>vitrinertite(V)> vitrite=clarite>vitrnertite(I)=inertite. Coal comprise about 5% of the sample and approximate maceral composition on mineral free basis: vitrinite 70%; inertinite 20%; liptinite 10%. Shaly coal rare, V>I>L, clarite>duroclarite=vitrinertite(I). Dom sparse, I>L>V. Inertinite and liptinite sparse, vitrinite rare. Mineral fluorescence weak orange. Iron oxides rare. Pyrite rare.)
1019.0m	$R_v$max	0.71	0.65-0.80	0.039	25	Abundant sporinite and common liptodetrinite orange
Core	$R_I$max	1.54	1.06-2.04	0.253	10	to dull orange, sparse cutinite orange, rare suberinite weak brown, rare resinite greenish yellow. (Shaly coal, V>I>L, clarite>duroclarite> inertite. Sample comprise exclusively of shaly coal and approximate maceral composition on mineral free basis: vitrinite 70%; inertinite 20%; liptinite 10%. Mineral fluorescence moderate to weak orange. Iron oxides rare. Pyrite rare.)
1104.2m	$R_v$max	0.83	0.70-0.90	0.043	25	Abundant sporinite and sparse liptodetrinite orange to
Core	$R_I$max	-	-	-	-	dull orange, common cutinite dull orange, common suberinite weak brown. (Coal, V>>L>I, clarite>vitrite. Sample comprise exclusively of coal consisting of clarite interbanded with vitrite. The approximate maceral composition of coal on mineral free basis: vitrinite 95%; liptinite 5%; inertinite traces. Mineral matter content of coal is high around 12% by volume. Mineral fluorescence moderate to strong orange. Iron oxides rare. Pyrite common.)
1535.0m	$R_v$max	0.79	0.67-0.88	0.042	25	Sparse sporinite and rare liptodetrinite dull orange to
Ctgs	$R_I$max	1.66	1.12-2.86	0.586	6	weak brown, rare cutinite dull orange. (Siltstone>claystone>shaly coal> coal>sandstone, Shaly coal abundant, V>>L>I, clarite>vitrite. Coal sparse, V>>L>I, clarite>vitrite. Dom sparse, L>I>V. Liptinite sparse, inertinite rare to sparse, vitrinite rare. Yellow fluorescing oil droplets in siltstone. Mineral fluorescence moderate to weak orange. Iron oxides rare. Pyrite sparse.)

VITRINITE REFLECTANCE MEASUREMENT

MEGASCOLIDES-1

Sample Details		Mean	Range	Std Dev	N° of Readings	Sample Description Including Liptinite Fluorescence, Maceral Abundances, Mineral Fluorescence
1820.0m Ctgs	$R_v$max	0.86	0.71-1.01	0.093	6	Rare sporinite and liptodetrinite dull orange to weak brown. (Siltstone>sandstone>claystone>shaly coal. Shaly coal rare, V>>L, clarite. Dom sparse, I>V. Inertinite sparse, vitrinite rare, liptinite absent. Mineral fluorescence weak dull orange to none. Iron oxides sparse. Pyrite rare.)
	$R_I$max	1.78	1.26-2.52	0.325	25	
1920.0m Core	$R_v$max	1.15	1.08-1.21	0.052	4	Fluorescing liptinite absent. (Siltstone. Dom common, I>>V.I>>V. Inertinite common, vitrinite rare, liptinite absent. Mineral fluorescence patchy moderate. Iron oxides rare. Pyrite sparse.)
	$R_I$max	1.91	1.46-2.60	0.278	25	

The shallow part of the section is early oil mature and a relatively rapid rise to late mature occurs by 1104.2 m. The deepest sample (1920 m and also core) shows a marked change in facies and a much higher vitrinite reflectance. In the deepest sample the vitrinite population is small and poorly defined relative to the remainder of the samples and indicates that the deepest section is close to the oil deadline. The two cuttings samples between 1104.2 m and 1920 m have similar levels of vitrinite reflectance to the core from 1104.2 m and could be influenced by the presence of cavings. The most probable interpretation is that the maturation level continues to rise below 1104.2 m reaching about 1.15% at 1920 m.

Coal is abundant in a number of the shallower samples and can be inferred to have good source potential. The deeper section is interpreted as having lower source potential.